ADVANCES
in
Austrian—Hungarian Joint Geological Research
Budapest, 1996

Thermal history of Austroalpine basement rocks of the borehole Fertőrákos-1004, Western Hungary

WOLFGANG FRANK, GYÖNGYI LELKES-FELVÁRI & ISTVÁN DUNKL*

Keywords: geochronology, fission track dating, Variscan and Alpine metamorphism, thermal history, borehole Fertőrákos-1004

Abstract

The borehole Fertőrákos-1004 offered an excellent opportunity for investigating a section of more than 1000 m of crystalline rocks near the Hungarian-Austrian boundary, where outcrops are rare and poorly preserved.

The lithological column studied shows more or less well preserved Variscan structures and metamorphic mineral assemblages in the lower part, made up of two-mica medium grained plagioclase gneisses with some amphibolite intercalations in the deepest portion. Alpine overprint is restricted to a fluid driven static alteration of plagioclase, formation of fine grained garnets and Ti loss from biotite laths.

The upper portion is characterized by fine grained phyllitic micaschists with strong Alpine penetrative overprint and some acid orthogneiss intercalations.

Rb/Sr (339±4, 287±3 Ma) and $^{39}Ar/^{40}Ar$ (>300 Ma) data from coarse grained white micas especially from the lower portion prove the Variscan metamorphism and cooling event. Biotites and partly also white micas which have been newly formed during early Alpine metamorphic overprint yielded $^{39}Ar/^{40}Ar$ ages mainly in the range 170–220 Ma. They show partly plateau type patterns with some rejuvenation. These ages are interpreted as strong arguments for the existence of surprisingly uniform ^{40}Ar overpressure during the formation of these micas. Only a few samples of biotites yielded Cretaceous $^{39}Ar/^{40}Ar$ age.

The existence of ^{40}Ar overpressure in large rock volumes at the time of deformation, mineral growth and cooling gives a strong argument that this argon overpressure was produced during nappe stacking in an active continental margin setting. In the course of this process frontal and cool parts of the Austroalpine crystalline (Wechsel unit) were dragged below the Semmering system, which has seen slightly higher thermal overprint and a distinctly more intense deformation.

The radiogenic argon released during this process was incorporated in most of the rocks of the Semmering system while cooling down from 450–300 °C, most probably in late Cretaceous times (biotite Rb/Sr 72 Ma).

A rapid cooling is indicated by somewhat older zircon fission track ages and mainly by apatite fission track ages about 43±2.3 Ma. This rapid cooling is correlated with a distinct uplift of the Wechsel dome during which several low-angle detachment faults were active.

Zusammenfassung

Die Tiefbohrung Fertőrákos-1004 bietet eine hervorragende Möglichkeit ein mehr als 1000 m mächtiges Profil im Kristallin entlang der ungarisch–österreichischen Grenze zu studieren, wo Aufschlüsse selten und schlecht erhalten sind.

Die lithologische Abfolge besteht im tieferen Teil aus mittelkörnigen Zweiglimmerplagioklasgneisen mit einigen Amphiboliteinschaltungen im tiefsten Bereich. Diese Gesteine weisen mehr oder weniger gut erhaltene variszische Strukturen und Mineral-Assoziationen auf. Die alpidische Überprägung ist durch eine fluidgesteuerte, statisch ablaufende Zersetzung der Plagioklase, Neubildung feinkörniger Granate, und Entmischung von Titanphasen in den Biotiten charakterisiert.

* Address of Authors: WOLFGANG FRANK, Laboratorium für Geochronologie und Isotopengeologie der BVFA, Franz Grill Str. 9, 1030 Vienna, Austria; GYÖNGYI LELKES-FELVÁRI, Hungarian Natural History Museum, Dept. of Mineralogy, 1083 Budapest, Ludovika tér 2; ISTVÁN DUNKL, Laboratory for Geochemical Research, Hungarian Academy of Sciences, 1112 Budapest, Budaőrsi u. 45

Der obere Teil des Profils besteht aus feinkörnigen phyllitischen Glimmerschiefern mit intensiver penetrativer alpidischer Durchbewegung und Einschaltungen einiger saurer Orthogneise.

Rb/Sr (339±4, 287±3 Ma) und $^{39}Ar/^{40}Ar$ (>300 Ma) Altersdaten von grobkörnigen Hellglimmern aus dem tieferen Abschnitt der Bohrung belegen ein variszisches Metamorphose- und Abkühlereignis. Biotite und z.T. auch Hellglimmer, die während der alpidischen Überprägung neugebildet wurden, haben $^{39}Ar/^{40}Ar$-Alterswerte zwischen 170 und 220 Ma ergeben. Sie zeigen teilweise plateauartige Altersdiagramme mit Verjüngungen im Niedrigtemperatur–Bereich. Diese Ergebnisse werden als klarer Hinweis auf einen überraschend einheitlichen Ar-Überschuss während der Neubildung dieser Glimmer gesehen. Nur wenige Biotite haben kretazische $^{39}Ar/^{40}Ar$ Alterswerte geliefert.

Das Vorhandensein von Ar-Überschuss in grossen Bereichen während Deformation, Mineralneubildung und Abkühlung liefert ein deutliches Argument dafür, dass dieser Ar-Überschuss während Deckenstapelung im Zuge der Ausbildung eines aktiven Kontinentalrandes stattfand. Im Zuge dieses Prozesses wurden frontale und kühle Teile des ostalpinen Kristallins (Wechselkristallin) unter das Semmeringsystem geschoben, das eine etwas höhere thermische Überprägung und deutlich intensivere Deformation aufweist. Das radiogene Ar, das im Zuge dieses Prozesses aus den tiefen Teilen freigesetzt wurde, wurde hauptsächlich im Kristallin des Semmeringsystems während seiner Abkühlung von 450–300°C eingebaut und zwar offensichtlich in spätkretazischer Zeit (Rb/Sr Biotit 72 Ma).

Eine weitere rasche Abkühlung ist hauptsächlich durch Apatit-Spaltspurenalter um 43±2.3 Ma und etwas ältere Zirkon-Spaltspurenalter dokumentiert.

Összefoglalás

A Fertőrákos-1004. sz. fúrás, amely a magyar–osztrák határ közelében mélyült, ahol csak kevés és rossz minőségű kibúvás van, kitűnő lehetőséget biztosított egy több, mint ezer méter vastag kristályos kőzetösszlet vizsgálatára.

A vizsgált kőzetoszlop alsó szakaszára, mely kétcsillámú középszemű plagioklászgneiszből áll, legalul néhány amfibolit közbetelepüléssel, többé-kevésbé jól megőrződött variszkuszi szerkezet és metamorf ásványegyüttes jellemző. Az alpi hatás csak a plagioklász fluidum-okozta statikus elváltozására, finomszemű gránát képződésére és a biotitlécek titán-vesztésére szorítkozik.

A felső szakaszra finomszemű fillites csillámpala jellemző, erőteljes penetratív alpi hatással és savanyú ortogneisz közbetelepülésekkel.

A Rb/Sr (339±4, 287±3 Ma) és $^{39}Ar/^{40}Ar$ (>300 Ma) kormeghatározások, amelyek durvaszemű fehér csillámokból készültek az alsó szakaszból, variszkuszi metamorfózist és lehűlést bizonyítanak. A kora-alpi metamorf hatásra újonnan képződött biotitok és részben fehér csillámok is 170–220 Ma időközbe eső koradatokat adtak. Részben plató-jellegű kordiagramot mutatnak némi megfiatalodással. Ezek a koradatok nyomós érvnek tekinthetők arra, hogy meglepően egyöntetű ^{40}Ar túlnyomás állt fenn e csillámok képződésekor. Csupán néhány biotitminta adott kréta kort.

^{40}Ar túlnyomás léte nagy kőzettömegekben a deformáció, ásványnövekedés és lehűlés idején határozottan amellett szól, hogy ez takarófeltolódás során, aktív kontinensszegélyen jött létre. Ennek folyamán az ausztroalpi kristályos (a Wechsel-egység) homloki és hideg részei vonszolódtak be a Semmering-rendszer alá, amely kissé erősebb hőhatást és határozottan erőteljesebb alakváltozást szenvedett. Az e folyamat során felszabadult radiogén argon jórészt a Semmering-rendszer kőzeteibe záródott be a 450–300 °C-ról való lehűlés során, minden valószínűség szerint az alsó krétában (Rb/Sr kor: 72 Ma).

Gyors lehűlésre utalnak a valamivel magasabb cirkon hasadásinyom-korok, valamint az apatit hasadásinyom-kora (kb. 43±2.3 Ma).

Introduction

To the SW of Lake Fertő (Neusiedler See), close to the boundary with Austria basement rocks outcrop in Hungary over an area of a few km^2. The basement rocks are highly weathered in the outcrops, however numerous drillings explored them to a depth of about 2000 m. Metamorphic rocks have a general dip to SE, the deepest portion plunges steeply to SE (70–80°) and upper horizons have a more gentle (20–25°) inclination. This basement is unconformably overlain by Miocene sediments. For the depositional age of the protoliths of these metamorphic rocks no fossil evidence is available.

The borehole Fertőrákos-1004 (FR) with a total depth of 1091 m crosscuts all the main rock units of this basement. The main tectonic units in the investigated area with the location of the borehole are shown in fig. 1. The main purpose of this study is to gain a better understanding of the metamorphic and uplift history of this basement by petrographical, geochronological and fission track methods and to correlate them with those of the surrounding areas.

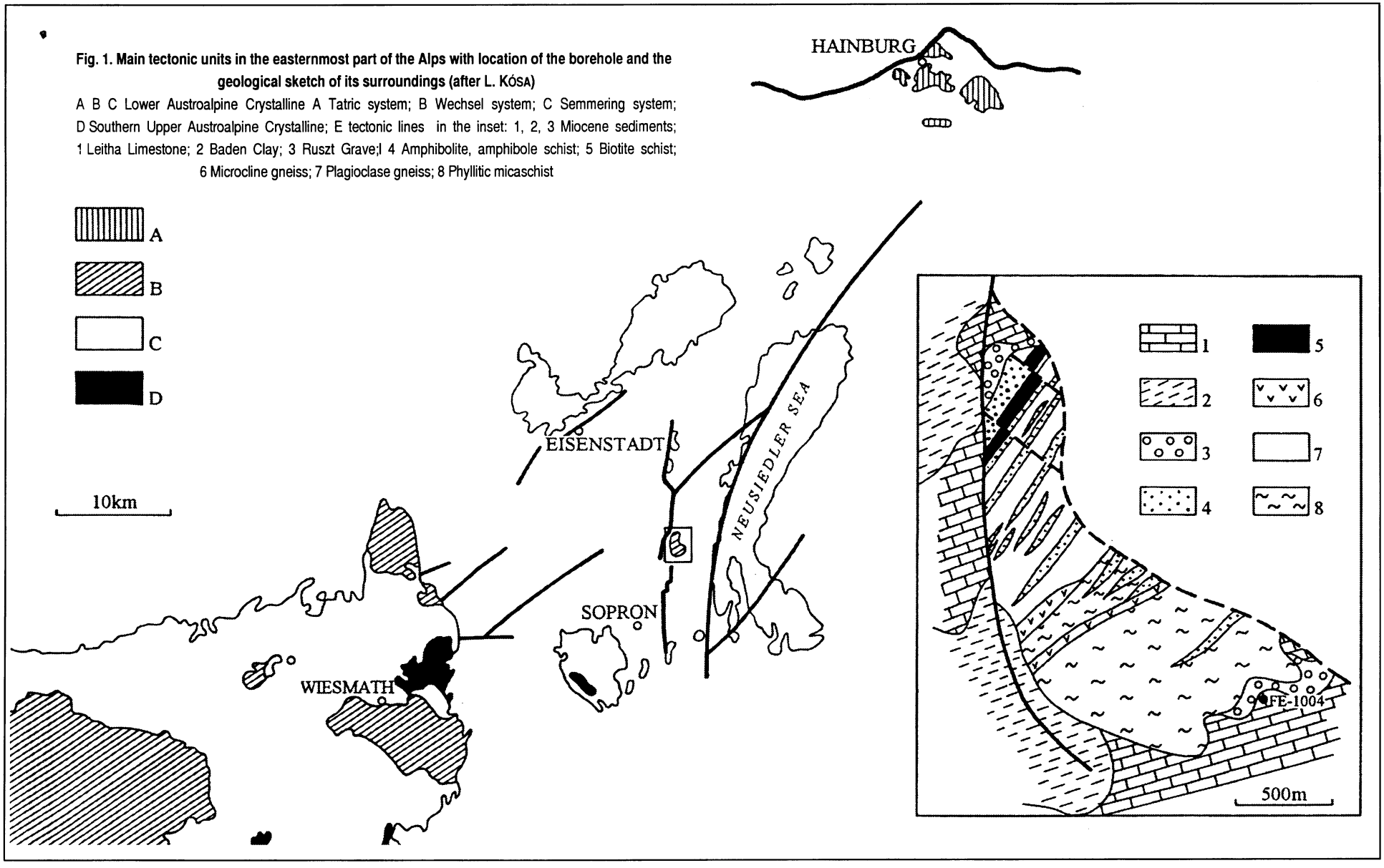

Fig. 1. Main tectonic units in the easternmost part of the Alps with location of the borehole and the geological sketch of its surroundings (after L. KÓSA)

A B C Lower Austroalpine Crystalline A Tatric system; B Wechsel system; C Semmering system; D Southern Upper Austroalpine Crystalline; E tectonic lines in the inset: 1, 2, 3 Miocene sediments; 1 Leitha Limestone; 2 Baden Clay; 3 Ruszt Grave;l 4 Amphibolite, amphibole schist; 5 Biotite schist; 6 Microcline gneiss; 7 Plagioclase gneiss; 8 Phyllitic micaschist

Geological setting

Eastern Lower Austroalpine units outcrop in Hungary near Sopron and Lake Fertő, with Miocene sedimentary cover. In the Sopron area acidic gneisses, different micaschists, metaquartzites and leukophyllites occur. LELKES-FELVÁRI et al. (1984) proposed a three-stage evolutional model for this basement, which is generally considered to belong to the Raabalpen or Semmering system (called also Grobgneiss or Kern Serie).

Near Lake Fertő metamorphic rocks are known mainly from boreholes. KÓSA & FAZEKAS (1976) differentiated three main units: a lower unit, made up of amphibolites and biotite schists, a middle feldspar bearing micaschist unit, with intercalations of amphibolites. Rocks of very high apatite content (up to 70–80%) make up lenses of a few tenth of cm in several horizons. High organic content in some metapelites is also characteristic. Phyllitic micaschists with intercalations of gneisses, marbles, metaquartzites and leukophyllites make up the uppermost unit. They correlated this basement with the Wechsel series, as described by FAUPL (1972).

In the Austrian part, granite gneisses and garnet-bearing retrogressed phyllitic micaschists outcropping near Mörbisch were considered by FUCHS (1965) to belong to the Kernserie and the albite-chlorite gneisses near Silberberg and Oslip to the Wechsel series.

As concerns the age of metamorphism of these units, from the Sopron area the following geochronologic data are available obtained by Rb/Sr method (KOVÁCH & SVINGOR 1988): — model ages of coarse-grained muscovites coming from muscovite gneisses in the range 205–281 Ma. — Fine-grained muscovites yielded 90–98 Ma. — Model ages of biotites from metagranites scatter in the range 41–55 Ma.

BALOGH & DUNKL (1994) carried out K/Ar dating, — coarse-grained muscovites from gneisses yielded age values in the range 109–160 Ma, fine-grained ones in the range 84–91 Ma.; biotites from metagranites fall in the range 79–101 Ma.

From the Fertőrákos area a Rb/Sr mineral isochron age of 351±9 Ma was obtained on coarse-grained muscovites; biotite ages scatter in the range 90–121 Ma. (KOVÁCH & SVINGOR 1981).

Structures and lithology

The lithological column of the borehole is shown in fig. 2. According to meso- and microscopic observations the metamorphic rocks belong to two different units both displaying polymetamorphic character; they are separated by thrust plains. The lower unit is a succession of interlayered medium-grained two-mica plagioclase gneisses and amphibolites, with subordinate amphibole gneisses and orthogneisses. In the upper unit phyllitic micaschists prevail with intercalated quartzphyllites, amphibolites and microcline augengneisses in three banks. Organic content is high in some levels. In general the two groups have tectonic contact at 460 m.

The main difference between these two units is the different deformational history during the Early Alpine stage of their metamorphic evolution. Microphotos of thin sections (figs 3, 4, 5) illustrate the textural variations.

In the lower unit pre-Alpine fabric is generally preserved (earlier metamorphic structures, and partly that of protoliths), minerals change their composition rather than distributions. New minerals are minute and do not change the earlier textures. Complete mineralogical-textural reorganization is restricted to thin shear zones.

In the upper unit ductile deformation and syntectonic recrystallization have resulted in a new penetrative schistosity in different rock-types. In some layers completely new structures developed. In others some of the overprinted structures survive: earlier foliations, remnant hinges of crenulation defined by mica orientations, inclusion trails in different minerals, distribution of an earlier mica generation. Beside microstructures relic mineral phases also occur.

However it would be too simple to interpret the whole section as a superposition of two individual units. The tectonism is more complicated. No intercalation of Permo–Mesozoic rocks was recognized, but there are several observations of tectonic intercalations of special lithologies which had a different metamorphic structural

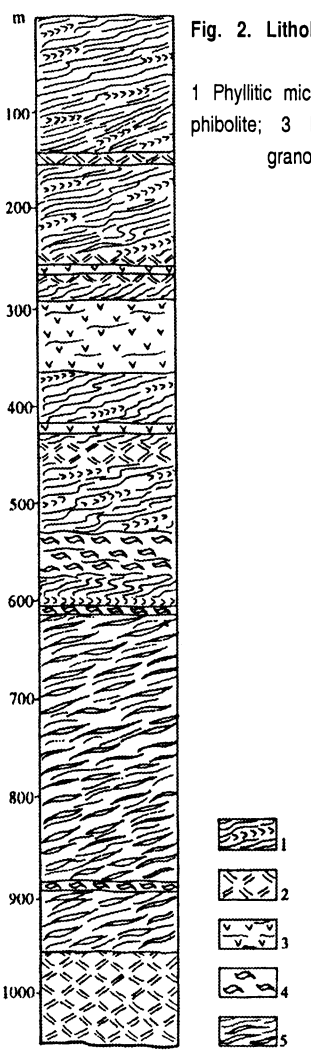

Fig. 2. Lithological column of the borehole FR-1004

1 Phyllitic micaschist; 2 Epidote-amphibolite, amphibolite; 3 Microcline augengneiss; 4 Metagranodiorite; 5 Plagioclase gneiss

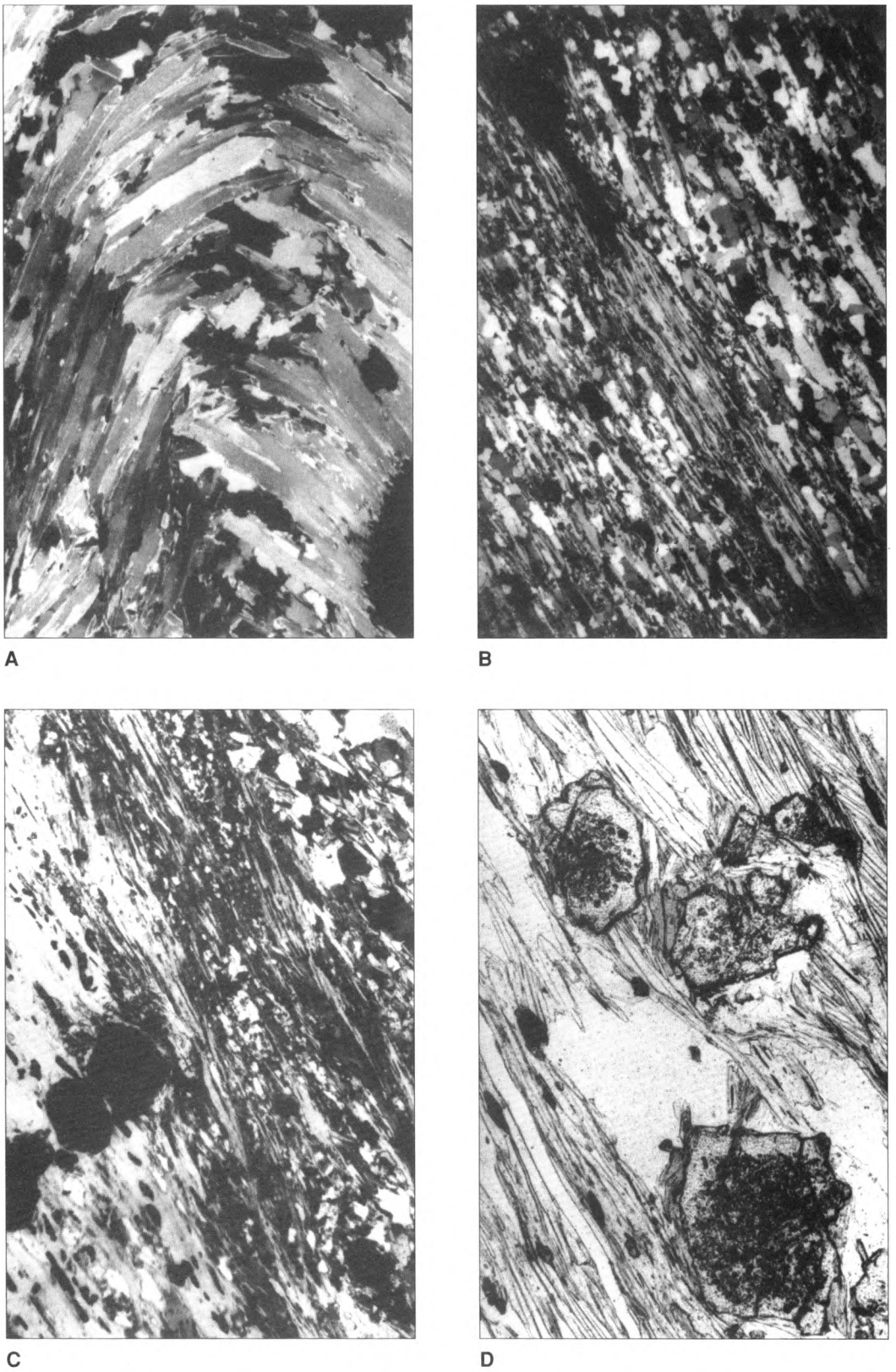

Fig. 3A–D

A. FR-1004 142 m, phyllitic micaschist. In hinge regions of relic crenulations mosaic of recrystallized micas replace bent bundle of crystals 32.5x B. FR-1004 186 m, garnet bearing biotite-muscovite phyllite. Subgrains with smooth grain boundaries in quartz ribbons. They are surrounded by a microcrystalline quartz+sericite+biotite+albite matrix. Coarser micas are dispersed or make up thin layers. 9.8x C. FR-1004 210 m, garnet bearing chlorite-muscovite schist. Garnet idioblasts and ilmenite needles set in a layer of coarse muscovite with a high degree of preferred orientation. Thin sheared layers are composed of quartz+albite+sericite+chlorite. 32.5x D. FR-1004 223 m, garnet and epidote bearing biotite-muscovite schist. Garnet idioblasts with incusion rich core and incusion free rims. A second phase of garnet growth on garnet crystal face outlined by opacitic dust (upper left). 65x

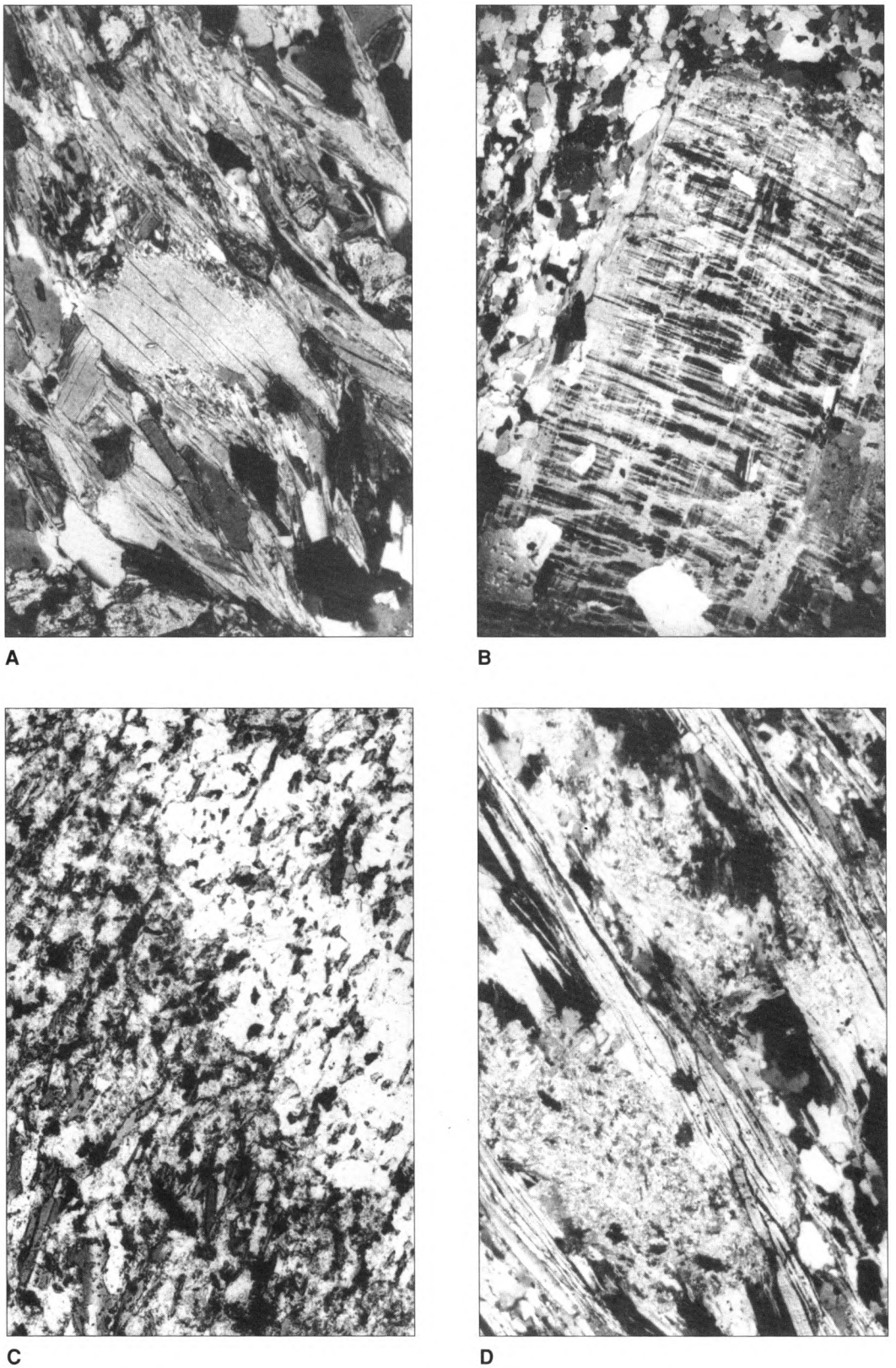

Fig. 4A–D

A. FR-1004 276 m, phyllitic micaschist. Coarse muscovite porphyroclast ("muscovite fish") with irregular grain boundaries with tails of cataclased and recrystallized fine grained mica. 65x; B. FR-1004 327 m, microcline augengneiss. Perthitic potash feldspar microaugen with albite and quartz inclusions set in a fine grained mosaic composed of quartz+albite+muscovite+biotite. 9.8x; C. FR-1004 609 m, biotite schist. Schistosity at a high angle to compositional layering. In quartz rich bands the grain size of biotite is smaller than in feldspar+biotite rich bands. Feldspar completely recrystallized in epidote+sericite. Biotite is crowded with opaque reaction products along margins of crystals. 32.5x; D. FR-1004 673 m, sericite pseudomorphs after plagioclase in muscovite gneiss. 32.5x

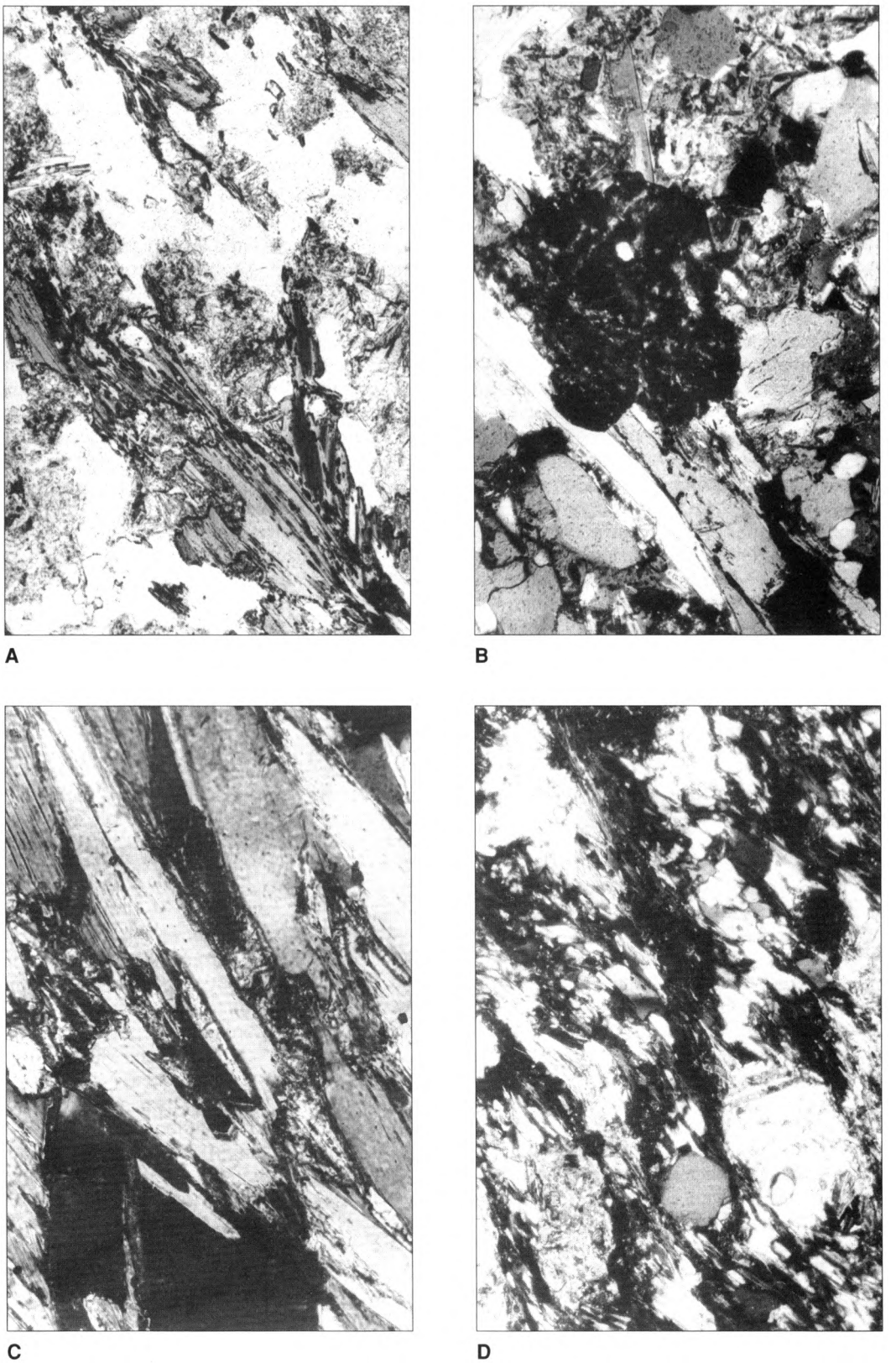

Fig. 5A-D

A. FR-1004 720 m, biotite-muscovite gneiss. Epidote+sericite+biotite+chlorite pseudomorphs after plagioclase. Biotite is partly chloritized with Fe-Ti exsolution along cleavage planes. 32.5x; B. FR-1004 745 m, biotite-muscovite gneiss. Sericite+biotite+quartz+garnet replace plagioclase. Garnet postdates muscovite-biotite crystal face. 65x; C. FFy 004 745 m, biotite-muscovite gneiss. Clinozoizite and sphene needles along biotite crystal margins. 130x; D. FR-1004 1094 m, albite-chlorite gneiss. Lens- shaped albite and polycrystalline quartz+albite lenses with assymmetrical pressure shadows in anastomosing seams of chlorite. 65x

history than the surroundings. Such intercalations occur at 400–460 m and at 609 m. It was not possible to deduce the detailed orientation of the linear fabric, because the drillcores had not been oriented. We think that a considerable part of the observed textures were formed during Cretaceous nappe stacking, but from comparison with neighbouring outcrops (e.g. Sopron area), we have to assume that several low-temperature shear zones and deformational features were formed in the prominent early Tertiary extensional phase.

Petrographic description of the analysed samples

184–186 m. Fine-grained biotite-muscovite phyllite. It has an entirely newly formed Alpine fabric. Its penetrative parallel foliation is expressed by elongated quartz+feldspar rich aggregates and mica-rich layers of highly preferred orientation. Phyllosilicates are also dispersed in the quartz+feldspar rich domains. Former plagioclase crystals recrystallized in albite, biotite, sericite and tiny euhedral garnets. Muscovite and biotite occur in two generations: a very fine-grained generation is associated to feldspars or appears as very thin layers around a coarser generation of micas. Garnets occur as deformed crystals with s_i to a high angle to s_e. They often have elongated pressure shadows composed of biotite and chlorite. Euhedral garnets together with the deformed ones often have inclusion-rich cores and inclusion-free rims. Garnet atolls with a central part composed of biotite+chlorite also occur. Accessory minerals are apatite, epidote, and sphene aggregates around ilmenite.

210 m. Muscovite quartz-phyllite. This is a fine grained layered rock with strong structural reworking. Muscovite laminae with a high degree of preferred orientation alternate with granoblastic quartz rich layers in a millimetric scale. The granoblastic layers are of various mineralogy: -albite+minor mica, -quartz, -quartz+mica, -quartz+albite+garnet. Chlorite and subordinately muscovite flakes are randomly oriented. The muscovite layers contain also a few randomly oriented muscovite and chlorite flakes, dispersed albite and garnet. The albite makes up small, inclusion-free idioblasts and more robust crystals with muscovite and chlorite inclusions, sometimes polycrystalline lenses. Garnet xeno -hypidioblasts have inclusion-rich core and inclusion-free rim. Late microshear zones resulting in grain size reduction, composed of quartz+sericite, are parallel with the main foliation.

276.4 m. Phyllitic biotite-muscovite micaschist with a slight layering and two distinct schistosity planes. The structure is dominated by a younger deformation-crystallization event. Quartz+albite bearing granoblastic layers and elongated lenses containing dispersed mica flakes alternate with arcuate lepidoblastic layers composed of muscovite and biotite, containing subordinate quartz and albite. They crosscut a faint older schistosity delineated by coarse, deformed muscovites of irregular grain boundaries. Albite sometimes have inclusion rich core and a clear rim. Chessboard albite also occur. Garnet suffered postcrystalline deformation, with chlorite, epidote and biotite in their pressure shadows. Dispersed euhedral epidote occur in micaceous layers.

325, 327–328 m. Microcline augengneiss. Micro-augens up to 1 cm (mainly 3–5 mm) are set in a fine-grained mosaic which is composed of quartz+ albite+microcline+muscovite+biotite. Microaugens are mainly polycrystalline twinned perthitic microclines (braid and string perthite) enclosing corroded or euhedral albite crystals with sericitic cores and xenoblastic quartz. Strongly sericitized albite makes up smaller microaugens. Thin, arcuate, anastomosing mica seams around augens are composed of decussate muscovite and subordinate biotite. More robust muscovite grains are dispersed in the groundmass or in the mica-rich seams, they are deformed, have irregular grain boundaries and contain small decussate muscovite flakes along grain boundaries. Garnet is present as small idioblasts in micas or plagioclase or make up glomeroblasts composed of small idioblasts or atoll-like crystals in quartz-rich domains. Sphene, apatite, zircon, epidote and carbonate are the accessory minerals.

609–610 m. Biotite gneiss. Compared to other lithologies, this rock exhibits a rather finegrained fabric. Biotite and feldspar rich layers are alternating in the scale of a few mm to a few cm of thickness. The grano- and lepidoblastic layers are slightly folded and an axial plane schistosity crosscuts at a high angle the compositional layering. Granoblastic layers are composed of quartz+albite+biotite. Lepidoblastic layers are made up of biotite and former plagioclase completely altered to sericite+epidote. A few muscovite flakes are intergrown with biotite. Biotite is bordered by tiny sphene idioblasts.

720, 742, 745, 747 m. Medium grained two-mica plagioclase gneiss. Structural reworking is restricted to very thin (0.1–0.2 mm) shear plains mostly parallel to the existing foliation. These Alpine deformational planes are visible only on the broken surfaces of the drillcores where coarse relictic mica flakes are visible in fine grained surfaces. This feature is practically invisible in thin section perpendicular to foliation. These rocks are slightly layered sometimes with microaugen texture, their penetrative foliation is slightly folded. Granoblastic composite quartz+feldspar spindle shaped grain aggregates or layers are surrounded by arcuate anastomosing mica rich layers. Mica occurs in dispersed flakes, too. Mica-rich layers are composed of decussate muscovite+biotite, they are slightly deformed, sometimes kinked. Biotite is bordered on intergranular faces by tiny sphene+epidote idioblasts, rutile+ilmenite appears along crystal faces and cleavage planes. Ilmenite is a stable mineral phase. Plagioclase recrystallized in sericite+epidote+biotite+ chlorite. Sometimes small garnet idioblasts can be observed in them. Garnet idioblasts also occur in mica-rich layers, their crystallization postdates mica/mica or mica/plagioclase interfaces. Recrystallized quartzitic lenses are bordered by chlorite. The chloritization of biotite and garnet is subordinate.

1072.3 m. Amphibolite. It has a relic gabbroic texture, coarse hornblende nematoblasts and plagioclase

make up the rock. Hornblende crystals often have actinolitic rims or actinolite+chlorite appears along cleavage planes or in intercrystalline places together with biotite. Albite+epidote+sericite replace plagioclase. Sometimes small garnet idioblasts occur in them. Sphene occurs as small, dispersed idioblasts or as aggregates around ilmenite.

Metamorphic grade

The metamorphic grade of the Alpine overprint corresponds in both units to greenschist facies. It reached a slightly higher temperature (400/450 °C max.) in the upper part, whereas it was usually distinctly less than 400 °C in the lower part, where preservation of the pre-Alpine mineralogy prevails for a considerable thickness (see "Discussion of age results"). It is obvious from the available sections that medium grade metamorphic rocks were the precursor lithologies in both units. The grade of this pre-Alpine metamorphic event can be characterized as high temperature greenschist to low amphibolite facies. It is a typical feature especially for the lower unit that except a few local occurrences, no pre-Alpine garnets have been found. Very fine garnet grains of obviously Alpine age can be observed within plagioclase or on grain boundaries of plagioclase and white mica. In the upper portion which is characterized by a distinctly more intense Alpine deformation/recrystallization, composite pre-Alpine/Alpine garnets occur in several thin sections. Single stage garnet porphyroblasts are a common feature in many lithologies there. No Al_2SiO_5 polymorphs or relics of them were observed. Only one example of randomly oriented white mica pseudomorphs after staurolite? was recognised in the upper part. From the microscopic observations low pressure type is indicated for the Variscan event.

Geochronology

The drillcores from FR-1004 offered the opportunity to study fresh material from an area where hardly any suitable material can be sampled. Earlier reconaissance investigations of some micas by the K/Ar method revealed ±Variscan white mica ages from the depth at 740 m and several white mica and biotite ages close to 180 Ma. We decided then to study the same samples with Ar/Ar method. Due to the limited number of samples and limited quantity of the mineral separates it was not possible to perform Ar/Ar and Rb/Sr-dating on the same minerals wherever it was desirable.

The term muscovite is used here for a white mica the composition of which has not been determined more precisely. We can rule out the widespread occurrence of paragonite which has not been detected by X-ray diffractometry. In the rocks which suffered a strong Alpine recrystallization the white mica can reasonably be considered a phengite.

Analytical procedure

Separation: mica concentrates processed in usual way were ground in an agate mortar mill to destroy mineral grains others than mica, to split up intergrown flakes and remove inclusions of apatite etc. For normal samples magnetic separation yields concentrates of typical purity around 99% and better. The mineral concentrates were enclosed in high purity quartz vials and irradiated at the 9MW ASTRA reactor at the Austrian Research Center Seibersdorf. Seven samples including one monitor are stored in a single level of a rotating sample holder, up to 5 levels were irradiated simultaneously. The usual duration for Variscan samples was 4 hours. After a cooling down period of at least three weeks the samples were filled in small, annealed (low blank) cylindrical tantalum capsules where the mineral grains are stored safely, but the released gas can move out through the small slit between bottom and cover measuring appr. 1 mm. The Ar extraction line presently in use is made of glass and fitted with a RF-heating furnace made from quartz glassware. The hot portion of the extraction furnace is double walled and this volume is continuously pumped to avoid diffusion from ambient air during the high temperature steps. Due to the geometry of the cylindrical tantalum capsules, which always have a horizontal position within the RF-induction spiral, a uniform temperature distribution in the sample is guaranteed. Temperatures are monitored by a calibrated pyrometer. The heating period is 10 minutes for the low temperature steps and is continuously lowered to 3 minutes at the high temperature steps.

Between the heating procedures the RF is switched off and no gas is released. The release patterns obtained with this procedure may thus not be completely reproduced by continuous heating experiments of the same samples, because thermal cycling may influence the diffusion characteristics of the mineral lattice. After measuring more than 400 samples of different ages, minerals and age-diagram patterns we can state that samples with uniform distribution of radiogenic Ar yield perfect plateau type patterns. Small disturbances in the samples are easier detected due to the reduced diffusion time for the single step. Samples with a strong thermal overprint or old cores — not incorporated in this investigation — seem to be characterised by more pronounced age variations derived from the individual domains compared to results of continuous diffusion experiments of longer duration.

Cleaning of the gas is done by a combination of cold traps and SAE-getters. To shorten the overall procedure time, no concentration of the Ar before sample inlet is made. 2/3 of the gas is introduced into the mass spectrometer, the VG-5400 model from FISONS ISOTOPES (Winsford, GB). The rest of the gas is pumped away from the extraction line. Isotopic ratios are determined from a measuring period of 10 min, representing the ratio at the time of sample inlet. Age calculation is done after corrections for mass discrimination and radioactive decay, especially of the ^{37}Ar, using the formulas given in DALRYMPLE 1984. The

specific production ratios of the interfering Ar isotopes at the ASTRA reactor of Seibersdorf are: $^{36}Ar/^{37}Ar(Ca)= 0.000_3$, $^{39}Ar/^{37}Ar(Ca)=0.000_65$, $^{40}Ar/^{39}Ar(K)=0.0_3$. The K/Ca ratio is determined from the $^{39}Ar/^{37}Ar$ ratio (calculated for the end of irradiation) using a conversion factor of 0.2_{47}. This factor was determined from a plagioclase with uniform and wellknown composition.

The line blank is rather low, at 1000 °C the ^{40}Ar blank is 2–5x10–10 cm^3 STP, the $^{40}Ar/^{36}Ar$ ratio of the line blank is similar to air composition. Interference of ^{36}Ar, ^{37}Ar, partly ^{39}Ar with a low background of hydrocarbon radicals in the mass spectrometer can be a limiting factor for reliable measurements of very low intensities. Carefully checked peak positions, background determination and corrections are routinely performed to overcome such difficulties. A full description of the technique used and the irradiation characteristics of the ASTRA-reactor in Seibersdorf is given in FRANK, CASTA, BICHLER and FRANK 1995 (in prep).

J values are determined with an internal laboratory standard, calibrated by international standards including muscovite Bern 4M (BURGHELE 1987; Chem. Geol.) and amphibole Mm1Hb. (SAMSON & ALEXANDER 1987). The errors given on the calculated age of an individual step include only the 1 s error of the analytical data. The error of the plateau ages or total gas ages include an additional error of ±0.4% on the J-value. Within these latter errors the age results are reproducible with the same analytical equipment. Interlaboratory reproducibility can be expected within 1–1.5%.

Results

Starting from the bottom of the borehole we obtained the following results (see fig. 6 and Table 1, 2, and 3).

1072 m. Biotite-bearing plagioclase amphibolite.

Handpicked amphibole separate yielded a typical staircase Ar/Ar pattern indicating a thermal overprint. More than 70% of the gas yielded typical Variscan step ages. There is a weak indication to a pre-Variscan age of relic domains in the amphibole.

747 m. Muscovite–plagioclase gneiss with preserved pre-Alpine structure.

Muscovite: coarse-grained flakes were separated.

Rb/Sr: 338,6±4 with a reasonable spread of 11.3

Table 1

Rb/Sr analytical results

SAMPLE		Sr ppm	Rb ppm	87Rb/86Sr	87Sr/86Sr±2sm	AGE
FR 184 m	WR	215	152	2.05	0.72559±5	
	Bi	14.7	606	121	0.84775±20	72.3±3 Ma
FR 210 m	WR	269	172	1.86	0.72703±8	due to low spread
	Mu fg	316	351	3.22	0.72735±5	no meaningful age
	Mu cg	374	337	2.62	0.72728±4	calculation possible
FR 327 m	WR	22.4	386	50.6	1.03211±7	
	Mu	5.39	1448	1161	5.66848±131	294±3 Ma
FR 745 m	WR	183	129	2.05	0.72274±4	
	Mu	63.8	207	9.45	0.75294±10	287±10 Ma
	Bi	4.67	444	288	1.16114±15	108± 3 Ma
FR 747 m	WR	187	148	2.30	0.72464±6	
	Mu	49.0	228	13.6	0.77911±4	339±12 Ma

Table 2

List of $^{39}Ar/^{40}Ar$ and Rb/Sr analytical results

SAMPLE	MIN	J-VALUE	ROCK TYPE	AGE	STEPS	%RAD	IC-AGE	40836 IC	COMMENT	Rb/Sr-AGE
FR 184 m	Mu	0.001655	biotite-muscovite phyllite	**195.8 ± 1.4 Ma**	plateau 12	99.8	...	...	disturbed pattern, excess Ar	
FR 184 m	Bi	0.005771	biotite-muscovite phyllite	**293.6 ± 1.7 Ma**	5–13 13	98.0	299 ± 9.5 **Ma**	43 ± 437	uniform excess Ar	Bi 72.3 +/-3 Ma
FR 210 m	Mu	0.004099	muscovite phyllite	**141.8 ± 1.4 Ma**	11	97.5	...		disturbed pattern, excess Ar	
FR 276 m	Mu	0.001655	phyllitic micaschist	**224.6 ± 1.6 Ma**	14	99.7	...	...	disturbed pattern, excess Ar	
FR 276 m	Bi	0.001655	phyllitic micaschist	**256.3 ± 1.6 Ma**	3–6 1	98.8	252 ± 5.2 **Ma**	371 ± 237	uniform excess Ar	
FR 325 m	Mu	0.005771	augengneiss	**98.3 ± 0.7 Ma**	11	96.6	100 ± 3 **Ma**	286 ± 146		
FR 325 m	Bi	0.005771	augengneiss	**93.2 ± 0.8 Ma**	5–12 1	98.4	93 5 ± 0.9 **Ma**	318 ± 91		
FR 327 m	Mu	0.004705	microcline augengneiss	**184.5 ± 1.0 Ma**	9–14 1	99.0	185 ± 1.4 **Ma**	273 ± 43	excess Ar	Mu 294+/-3 Ma
FR 609 m	Bi	0.004852	finegrained biotite gneiss	**179.0 ± 1.4 Ma**	2–10 1	97.9	180 ± 3.9 **Ma**	256 ± 201	excess Ar	
FR 720 m	Mu	0.004949	plagioclase gneiss	**240.0 ± 3.7 Ma**	11	97.5	...	...	partially reset	
FR 720 m	Bi	0.004945	plagioclase gneiss	**171.3 ± 2.1 Ma**	2–12 1	96.4	172 ± 1.8 **Ma**	493 ± 49	partially reset?, excess Ar?	
FR 742 m	Mu	0.004949	plagioclase gneiss	**301.0 ± 2.2 Ma**	16	99.2	...	...	slightly reset	
FR 745 m	Mu	0.004949	plagioclase gneiss	**305.4 ± 2.0 Ma**	16	99.3	...	...	slightly reset	Mu 287+/-3 Ma,
FR 745 m	Bi	0.004949	plagioclase gneiss	**213.5 ± 2.0 Ma**	2–13 1	98.0	214 ± 1.8 **Ma**	354 ± 28	partially reset, excess Ar?	Bi 108+/-1 Ma
FR 747 m	Mu	0.004705	plagioclase gneiss	**305.4 ± 1.8 Ma**	12	99.2	...	...	partially reset	Mu 339+/-4 Ma
FR 1072 m	Hbl	0.004750	amphibolite	**344.0 ± 12 Ma**	9	90.0	...	...	polyphase history	

A) FR 184 m; MUSCOVITE, biotite–muscovite phyllite (J = 0.001655 ± 0.4%)

Step	T[°C]	%39	40*	%rad	39/37	%36Ca	40*/39	age
1	630	1.0%	63.36 mV	96.0%	33	0.11%	60.80 ± 4.0%	180.7 ± 6.9
2	650	2.7%	169.06 mV	97.8%	65	0.11%	59.51 ± 0.6%	177.1 ± 1.1
3	680	3.3%	207.17 mV	98.3%	62	0.15%	59.60 ± 0.4%	177.3 ± 0.6
4	700	9.5%	639.79 mV	98.4%	99	0.09%	63.77 ± 0.2%	189.1 ± 0.4
5	725	20.0%	1553.76 mV	99.4%	118	0.18%	73.14 ± 0.2%	215.4 ± 0.4
6	750	12.2%	826.70 mV	99.4%	101	0.27%	63.77 ± 0.1%	189.1 ± 0.2
7	780	10.1%	642.09 mV	98.9%	94	0.15%	59.99 ± 0.3%	178.4 ± 0.5
8	820	10.0%	636.59 mV	99.0%	97	0.16%	59.99 ± 0.1%	178.4 ± 0.2
9	840	11.6%	817.68 mV	99.3%	94	0.23%	66.53 ± 0.3%	196.9 ± 0.6
10	870	6.9%	506.24 mV	99.7%	53	0.96%	68.86 ± 0.4%	203.4 ± 0.8
11	920	6.5%	478.85 mV	99.8%	56	1.15%	69.91 ± 0.6%	206.4 ± 1.1
12	1020	6.3%	477.53 mV	98.3%	50	0.15%	71.39 ± 0.3%	210.5 ± 0.5
							total gas age:	195.8 ± 1.4

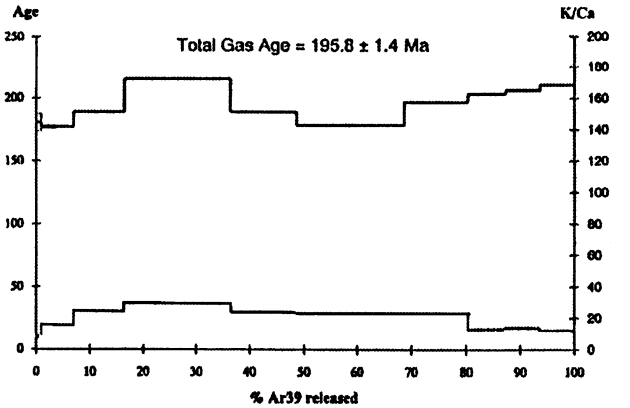

B) FR 184 m; BIOTITE, phyllitic micaschist (J = 0.005771 ± 0.4%)

Step	T[°C]	%39	40*	%rad	39/37	%36Ca	40*/39	age
1	670	0.9%	125.46 mV	62.8%	61	0.01%	23.99 ± 0.6%	244.4 ± 1.3
2	690	2.1%	331.77 mV	77.8%	123	0.01%	27.08 ± 0.2%	273.7 ± 0.6
3	710	4.2%	692.45 mV	88.5%	190	0.01%	27.93 ± 0.1%	281.7 ± 0.2
4	740	4.8%	794.33 mV	95.6%	211	0.03%	28.39 ± 0.1%	286.0 ± 0.3
5¹	760	9.9%	1673.03 mV	97.0%	264	0.04%	28.79 ± 0.1%	289.7 ± 0.4
6¹	820	7.5%	1269.94 mV	97.6%	331	0.04%	28.79 ± 0.1%	289.8 ± 0.3
7¹	840	10.7%	1813.72 mV	97.9%	253	0.06%	28.84 ± 0.1%	290.2 ± 0.3
8¹	870	3.7%	637.17 mV	98.0%	227	0.07%	29.33 ± 0.3%	294.7 ± 0.7
9¹	915	5.8%	975.26 mV	98.0%	121	0.13%	28.83 ± 0.1%	290.2 ± 0.3
10¹	960	20.1%	3442.75 mV	98.1%	165	0.10%	29.31 ± 0.1%	294.6 ± 0.2
11¹	1000	9.1%	1553.41 mV	97.7%	107	0.13%	29.24 ± 0.1%	293.9 ± 0.3
12¹	1060	16.7%	2902.07 mV	97.9%	142	0.11%	29.75 ± 0.1%	298.7 ± 0.2
13¹	1120	4.5%	781.96 mV	97.6%	262	0.05%	29.47 ± 0.2%	296.1 ± 0.4
							total gas age:	291.9 ± 1.9
						88%	¹plateau age:	293.6 ± 1.7

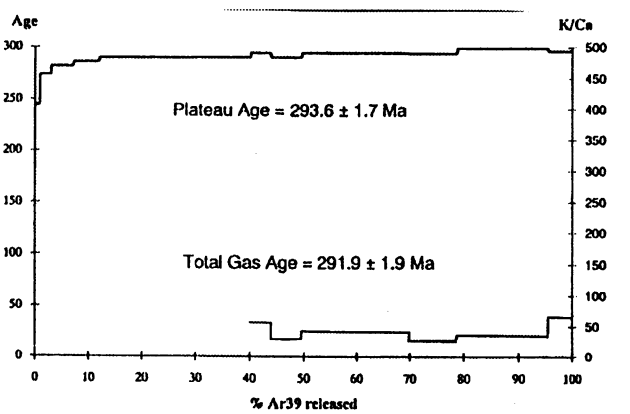

C) FR 210 m; MUSCOVITE, muscovite phyllite (J = 0.004099 ± 0.4%)

Step	T[°C]	%39	40*	%rad	39/37	%36Ca	40*/39	age
1	780	1.1%	25.79 mV	82.4%	41	0.07%	14.62 ± 1.2%	109.7 ± 1.2
2	810	5.7%	160.08 mV	83.9%	47	0.06%	16.98 ± 0.5%	126.8 ± 0.6
3	850	39.9%	1443.80 mV	97.5%	52	0.33%	21.77 ± 0.1%	161.1 ± 0.1
4	890	7.5%	183.81 mV	96.3%	34	0.49%	14.70 ± 0.4%	110.3 ± 0.4
5	940	6.3%	150.44 mV	94.1%	21	0.49%	14.44 ± 0.4%	108.4 ± 0.5
6	970	10.5%	258.39 mV	95.9%	42	0.35%	14.83 ± 0.2%	111.2 ± 0.3
7	1010	6.5%	176.96 mV	96.9%	42	0.43%	16.42 ± 0.3%	122.8 ± 0.4
8	1050	7.1%	229.78 mV	96.9%	35	0.43%	19.47 ± 0.4%	144.8 ± 0.5
9	1080	6.1%	214.13 mV	97.0%	35	0.41%	21.03 ± 0.2%	155.9 ± 0.3
10	1120	6.1%	227.65 mV	94.8%	25	0.30%	22.44 ± 0.1%	165.9 ± 0.2
11	1190	3.4%	103.10 mV	47.6%	15	0.03%	18.36 ± 1.2%	136.7 ± 1.6
							total gas age:	141.8 ± 1.4

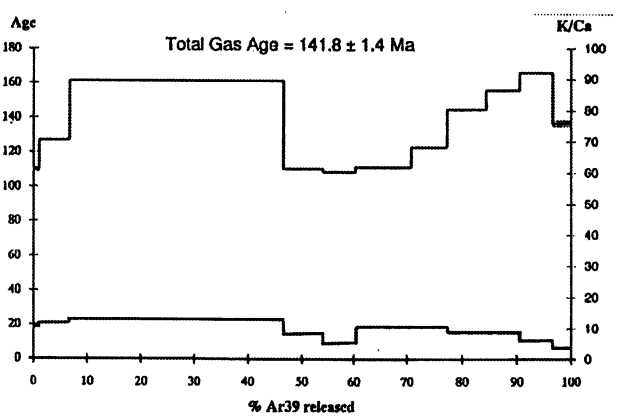

Fig. 6 (A, B, C) Ar/Ar plots

D) FR 276 m; MUSCOVITE, phyllitic micaschist (J = 0.001655 ± 0.4%)

Step	T[°C]	%39	40*	%rad	39/37	%36Ca	40*/39	age
1	620°	2.7%	306.76 mV	84.2%	18	0.04%	58.53 ± 0.8%	174.3 ± 1.4
2	650°	1.0%	128.08 mV	97.2%	62	0.08%	67.08 ± 0.3%	198.5 ± 0.6
3	670°	4.1%	542.49 mV	97.7%	280	0.02%	67.98 ± 0.6%	201.0 ± 1.2
4	690°	7.3%	971.27 mV	97.9%	260	0.02%	68.85 ± 0.3%	203.4 ± 0.5
5	710°	4.1%	571.77 mV	97.8%	328	0.02%	72.31 ± 0.3%	213.1 ± 0.6
6	725°	12.3%	1947.15 mV	98.1%	536	0.01%	81.73 ± 0.2%	239.1 ± 0.4
7	750°	7.2%	1149.55 mV	99.0%	504	0.02%	82.96 ± 0.2%	242.5 ± 0.5
8	780°	23.6%	3435.44 mV	99.0%	554	0.02%	75.22 ± 0.1%	221.2 ± 0.3
9	820°	11.9%	1652.21 mV	98.2%	588	0.01%	71.69 ± 0.1%	211.4 ± 0.2
10	860°	11.5%	1758.94 mV	98.2%	373	0.02%	79.24 ± 0.2%	232.3 ± 0.4
11	880°	8.8%	1421.26 mV	99.1%	352	0.03%	83.06 ± 0.2%	242.8 ± 0.5
12	910°	2.0%	341.85 mV	99.5%	150	0.15%	88.62 ± 0.1%	258.0 ± 0.2
13	960°	1.5%	243.13 mV	99.1%	144	0.08%	85.05 ± 1.7%	248.2 ± 4.0
14	1040°	2.0%	324.42 mV	99.0%	460	0.02%	84.80 ± 0.5%	247.6 ± 1.2
							total gas age:	224.6 ± 1.6

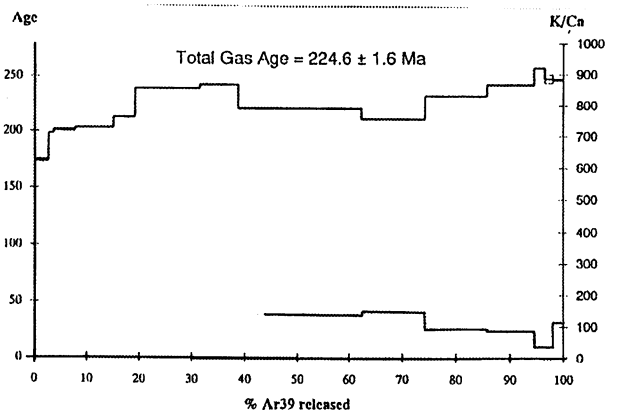

E) FR 276 m; BIOTITE, phyllitic micaschist (J = 0.005771 ± 0.4%)

Step	T[°C]	%39	40*	%rad	39/37	%36Ca	40*/39	age
1	570	1.1%	57.69 mV	69.5%	36	0.01%	58.45 ± 2.4%	174.1 ± 4.1
2	580	3.0%	208.98 mV	88.0%	139	0.01%	79.34 ± 1.2%	232.6 ± 2.5
3¹	600	6.6%	506.51 mV	95.1%	758	0.00%	87.72 ± 0.1%	255.5 ± 0.2
4¹	620	19.1%	1473.15 mV	98.0%	626	0.01%	88.18 ± 0.2%	256.8 ± 0.5
5¹	640	14.9%	1143.58 mV	98.6%	600	0.01%	87.48 ± 0.2%	254.9 ± 0.5
6¹	680	20.3%	1569.58 mV	98.8%	671	0.01%	88.32 ± 0.1%	257.2 ± 0.3
7	700	8.2%	598.91 mV	97.6%	578	0.01%	83.25 ± 0.3%	243.3 ± 0.6
8	730	9.4%	707.02 mV	98.6%	340	0.02%	86.20 ± 0.4%	251.4 ± 0.9
10	850	10.4%	761.60 mV	98.7%	29	0.30%	83.82 ± 1.6%	244.9 ± 3.7
11	920	6.5%	506.20 mV	98.0%	69	0.07%	88.57 ± 0.2%	257.8 ± 0.4
12	1040	0.5%	35.61 mV	91.6%	79	0.02%	79.31 ± 3.1%	232.5 ± 6.8
							total gas age:	251.9 ± 2.2
						61%	¹plateau age:	256.3 ± 1.6

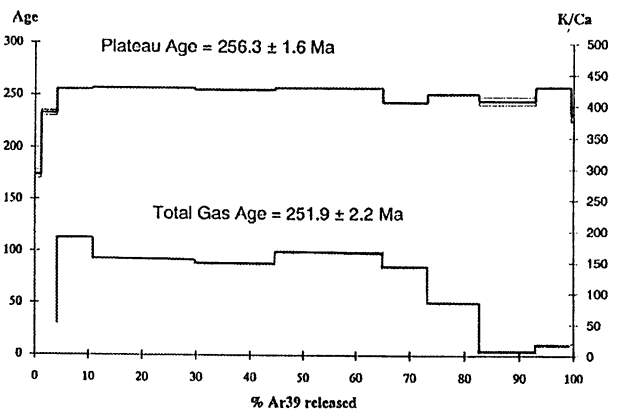

F) FR 325 m; MUSCOVITE, augengneiss (J = 0.004099 ± 0.4%)

Step	T[°C]	%39	40*	%rad	39/37	%36Ca	40*/39	age
1	680	1.0%	68.92 mV	84.4%	80	0.08%	8.08 ± 0.4%	85.9 ± 0.3
2	710	1.6%	110.60 mV	89.7%	200	0.05%	8.60 ± 0.4%	91.3 ± 0.3
3	760	1.9%	134.06 mV	92.9%	280	0.05%	8.77 ± 0.1%	93.0 ± 0.1
4	790	5.1%	382.85 mV	93.4%	324	0.04%	9.16 ± 0.1%	97.1 ± 0.1
5	835	7.5%	583.66 mV	89.0%	669	0.01%	9.56 ± 0.1%	101.2 ± 0.1
6	860	17.9%	1383.49 mV	94.8%	1137	0.02%	9.49 ± 0.0%	100.5 ± 0.0
7	890	23.4%	1711.56 mV	95.6%	1580	0.01%	9.01 ± 0.1%	95.5 ± 0.1
8	940	20.3%	1493.92 mV	95.6%	1794	0.01%	9.03 ± 0.1%	95.8 ± 0.1
9	980	11.6%	920.06 mV	96.5%	742	0.04%	9.72 ± 0.1%	102.9 ± 0.1
10	1000	5.5%	431.96 mV	96.4%	224	0.12%	9.66 ± 0.2%	102.3 ± 0.2
11	1100	4.1%	318.34 mV	96.5%	77	0.36%	9.65 ± 0.1%	102.2 ± 0.1
							total gas age:	98.3 ± 0.7

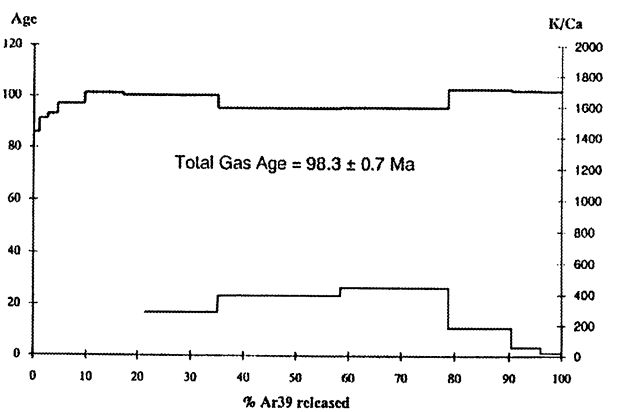

Fig. 6 (D, E, F) Ar/Ar plots

G) FR 325 m; BIOTITE, augengneiss (J = 0.005771 ± 0.4%)

Step	T[°C]	%39	40*	%rad	39/37	%36Ca	40*/39	age
1	650	0.4%	11.58 mV	65.9%	115	0.03%	5.79 ± 2.2%	61.9 ± 1.4
2	680	1.0%	35.65 mV	77.3%	110	0.04%	7.00 ± 1.1%	74.7 ± 0.8
3	700	2.3%	99.30 mV	87.1%	112	0.07%	8.44 ± 1.3%	89.6 ± 1.1
4	720	2.2%	100.54 mV	94.0%	381	0.05%	8.63 ± 0.5%	91.6 ± 0.4
5¹	750	6.9%	315.77 mV	96.4%	446	0.07%	8.73 ± 0.4%	92.6 ± 0.4
6¹	780	9.2%	419.88 mV	97.7%	504	0.10%	8.77 ± 0.6%	93.0 ± 0.6
7¹	800	6.1%	280.64 mV	97.5%	528	0.09%	8.78 ± 0.5%	93.1 ± 0.5
8¹	835	8.6%	393.52 mV	97.1%	569	0.07%	8.79 ± 0.4%	93.3 ± 0.3
9¹	880	13.8%	634.54 mV	97.3%	457	0.09%	8.86 ± 0.4%	94.0 ± 0.4
10¹	930	25.9%	1182.16 mV	98.1%	444	0.15%	8.77 ± 0.2%	93.1 ± 0.2
11¹	980	15.6%	710.39 mV	98.4%	330	0.24%	8.77 ± 0.4%	93.0 ± 0.4
12¹	1030	6.3%	288.36 mV	98.0%	174	0.35%	8.84 ± 0.4%	93.8 ± 0.4
13	1100	1.8%	75.65 mV	95.4%	82	0.31%	8.05 ± 0.7%	85.6 ± 0.6
							total gas age:	92.7 ± 0.9
						92%	¹plateau age:	93.2 ± 0.8

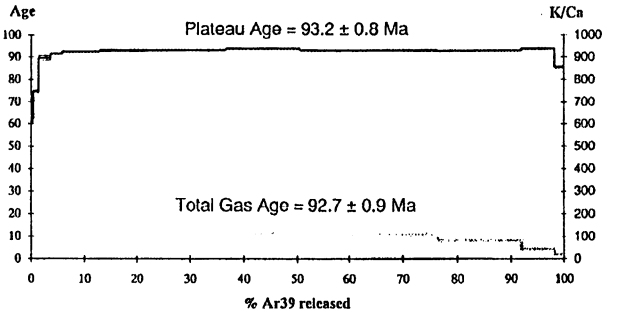

H) FR 327 m; MUSCOVITE, microcline–augengneiss (J = 0.004705 ± 0.4%)

Step	T[°C]	%39	40*	%rad	39/37	%36Ca	40*/39	age
1	580	0.1%	11.26 mV	72.5%	39	0.04%	16.83 ± 6.3%	143.6 ± 8.7
2	600	0.1%	11.94 mV	81.1%	88	0.02%	18.89 ± 1.5%	160.5 ± 2.3
3	610	0.3%	29.90 mV	88.7%	294	0.01%	19.00 ± 1.0%	161.4 ± 1.6
4	620	0.7%	63.49 mV	93.4%	719	0.01%	20.63 ± 0.8%	174.6 ± 1.4
5	630	0.8%	80.52 mV	95.2%	718	0.01%	20.79 ± 0.4%	175.9 ± 0.7
6	640	0.8%	71.63 mV	96.6%	562	0.02%	20.07 ± 0.7%	170.1 ± 1.1
7	650	1.8%	172.46 mV	96.3%	692	0.02%	20.49 ± 0.4%	173.5 ± 0.7
8	680	3.2%	310.48 mV	95.2%	660	0.01%	21.09 ± 0.3%	178.3 ± 0.5
9¹	700	6.5%	656.46 mV	96.8%	1065	0.01%	21.67 ± 0.1%	183.0 ± 0.2
10¹	720	50.0%	5095.27 mV	98.6%	1814	0.02%	21.89 ± 0.1%	184.7 ± 0.1
11¹	770	6.5%	650.37 mV	98.4%	1560	0.02%	21.66 ± 0.2%	182.9 ± 0.3
12¹	830	17.7%	1803.36 mV	99.0%	1594	0.03%	21.91 ± 0.1%	184.9 ± 0.1
13¹	860	4.4%	444.84 mV	97.7%	455	0.04%	21.90 ± 0.1%	184.8 ± 0.2
14¹	910	2.8%	280.61 mV	94.3%	243	0.03%	21.77 ± 0.2%	183.9 ± 0.4
15	960	1.1%	111.65 mV	89.8%	223	0.02%	21.46 ± 0.5%	181.3 ± 0.9
16	1060	3.2%	321.60 mV	94.2%	301	0.02%	21.54 ± 0.2%	182.0 ± 0.4
							total gas age:	183.6 ± 1.1
						88%	¹plateau age:	184.5 ± 1.0

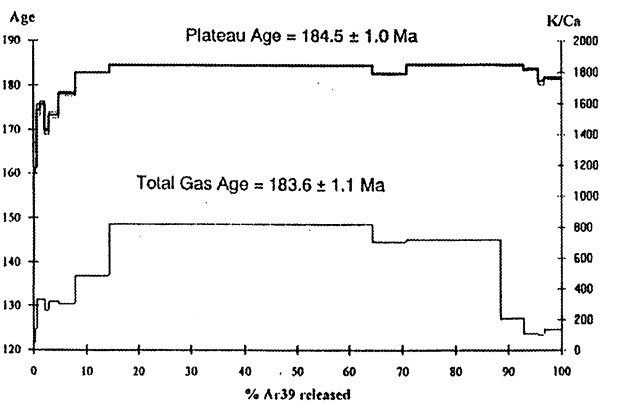

I) FR 609 m; BIOTITE, fine-grained biotite gneiss (J = 0.004746 ± 0.4%)

Step	T[°C]	%39	40*	%rad	39/37	%36Ca	40*/39	age
1¹	580°	2.5%	331.98 mV	74.8%	31	0.05%	15.69 ± 0.4%	135.3 ± 0.5
2¹	590°	6.0%	1014.04 mV	93.7%	71	0.10%	20.00 ± 0.1%	170.9 ± 0.2
3¹	600°	1.2%	212.04 mV	95.1%	111	0.08%	20.31 ± 0.3%	173.5 ± 0.5
4¹	620°	5.6%	979.66 mV	97.4%	138	0.12%	20.62 ± 0.2%	176.0 ± 0.3
5¹	640°	6.7%	1164.59 mV	97.0%	132	0.11%	20.61 ± 0.1%	175.9 ± 0.2
6¹	720°	10.0%	1769.23 mV	97.8%	145	0.14%	21.03 ± 0.0%	179.3 ± 0.1
8¹	730°	4.1%	719.62 mV	97.4%	134	0.12%	20.93 ± 0.2%	178.6 ± 0.3
9¹	740°	2.4%	432.36 mV	98.2%	143	0.17%	21.26 ± 5.2%	181.2 ± 9.0
10¹	780°	15.7%	2618.80 mV	98.1%	93	0.27%	19.79 ± 0.1%	169.2 ± 0.2
11¹	810°	15.3%	2720.47 mV	98.1%	81	0.29%	21.15 ± 0.2%	180.3 ± 0.3
12¹	950°	30.4%	5349.66 mV	98.5%	86	0.36%	20.90 ± 0.1%	178.3 ± 0.1
							total gas age:	175.5 ± 1.3

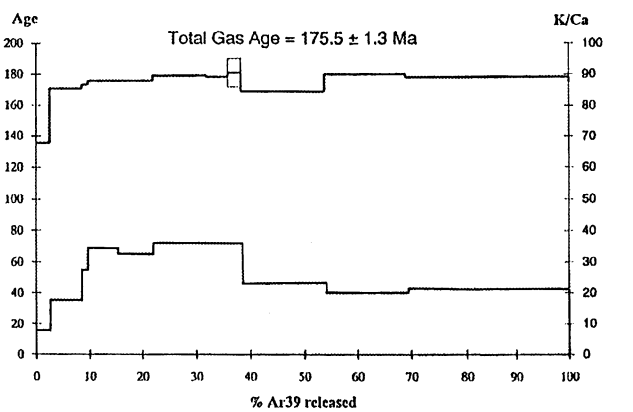

Fig. 6 (G, H, I) Ar/Ar plots

J) FR 720 m; MUSCOVITE, plagioclase gneiss (J = 0.004949 ± 0.4%)

Step	T[°C]	%39	40*	%rad	39/37	%36Ca	40*/39	age
1	670	1.7%	132.02 mV	66.7%	62	0.02%	18.94 ± 2.5%	168.9 ± 4.1
3	700	1.7%	148.84 mV	68.9%	22	0.04%	20.88 ± 10.4%	185.3 ± 18.3
4	750	10.8%	1141.06 mV	91.3%	115	0.03%	25.70 ± 1.8%	225.7 ± 3.8
5	800	33.4%	3918.80 mV	98.0%	246	0.06%	28.60 ± 1.0%	249.6 ± 2.4
6	830	15.3%	1210.71 mV	93.9%	181	0.04%	19.37 ± 1.2%	172.6 ± 2.0
7	850	4.8%	517.40 mV	97.1%	231	0.05%	26.13 ± 0.4%	229.3 ± 0.8
8	900	8.0%	989.30 mV	98.0%	281	0.05%	30.25 ± 0.1%	263.0 ± 0.3
9	930	15.3%	1996.25 mV	98.8%	274	0.09%	31.79 ± 0.1%	275.4 ± 0.4
10	980	5.1%	676.37 mV	97.5%	264	0.04%	32.36 ± 0.2%	280.0 ± 0.6
12	1000	2.6%	354.82 mV	90.1%	142	0.02%	33.47 ± 0.6%	288.9 ± 1.5
13	1100	1.2%	163.64 mV	66.5%	39	0.01%	33.74 ± 2.9%	291.1 ± 7.8
							total gas age:	239.9 ± 3.7

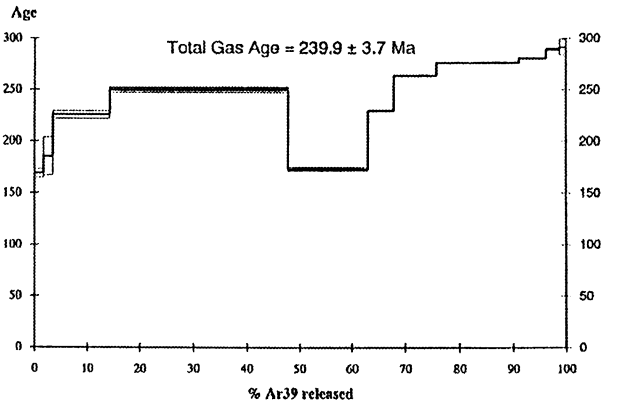

K) FR 720 m; BIOTITE, plagioclase gneiss (J = 0.004945 ± 0.4%)

Step	T[°C]	%39	40*	%rad	39/37	%36Ca	40*/39	age
1	640	3.7%	225.59 mV	62.8%	63	0.03%	15.32 ± 1.3%	137.7 ± 1.7
2'	650	8.2%	626.47 mV	87.6%	478	0.01%	19.24 ± 0.3%	171.3 ± 0.5
3'	680	4.2%	331.25 mV	92.5%	621	0.02%	19.63 ± 0.2%	174.6 ± 0.3
4'	700	7.7%	592.93 mV	94.9%	757	0.02%	19.36 ± 0.3%	172.3 ± 0.5
5'	720	6.1%	473.20 mV	95.9%	858	0.02%	19.37 ± 0.1%	172.4 ± 0.2
6'	750	4.2%	321.03 mV	95.8%	851	0.02%	19.33 ± 0.6%	172.1 ± 0.9
7'	800	6.6%	506.60 mV	96.4%	833	0.03%	19.25 ± 0.4%	171.4 ± 0.6
8'	830	3.4%	241.37 mV	93.9%	897	0.01%	17.97 ± 2.8%	160.4 ± 4.3
9'	870	11.2%	875.41 mV	68.4%	196	0.01%	19.68 ± 0.3%	175.0 ± 0.5
10'	900	1.3%	96.01 mV	95.9%	123	0.15%	19.02 ± 0.3%	169.5 ± 0.5
11'	960	30.0%	2289.66 mV	94.6%	335	0.04%	19.13 ± 0.1%	170.3 ± 0.1
12'	1000	13.5%	1027.93 mV	89.2%	33	0.19%	19.16 ± 0.2%	170.6 ± 0.3
							total gas age:	170.0 ± 2.2
				96%			'plateau age:	171.3 ± 2.1

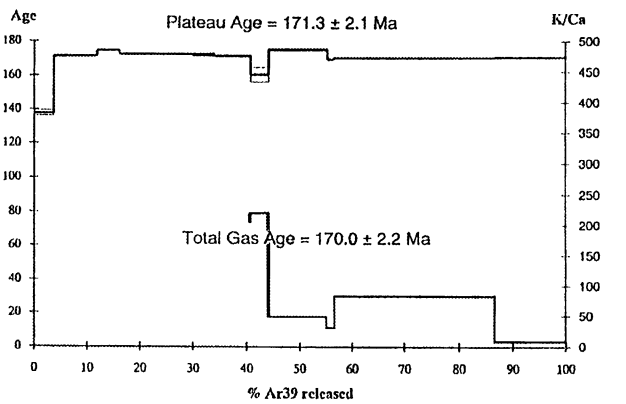

L) FR 742 m; MUSCOVITE, plagiclase gneiss (J = 0.004949 ± 0.4%)

Step	T[°C]	%39	40*	%rad	39/37	%36Ca	40*/39	age
1		1.3%	74.08 mV	77.3%	42	0.03%	29.05 ± 2.1%	253.2 ± 5.0
2		0.5%	34.39 mV	92.2%	226	0.01%	33.39 ± 2.4%	288.3 ± 6.3
3	650	0.3%	20.86 mV	91.5%	331	0.01%	33.44 ± 2.9%	288.7 ± 7.7
4	660	1.5%	93.60 mV	93.6%	341	0.01%	32.17 ± 0.5%	278.5 ± 1.2
5	680	2.1%	133.02 mV	95.7%	459	0.01%	32.36 ± 0.8%	280.0 ± 2.0
6	700	2.8%	192.01 mV	96.5%	550	0.01%	33.86 ± 0.5%	292.1 ± 1.4
7	730	4.1%	277.56 mV	97.7%	710	0.02%	33.52 ± 0.2%	289.3 ± 0.6
8	750	7.0%	488.37 mV	98.1%	1174	0.01%	35.13 ± 0.2%	302.2 ± 0.6
9	780	12.0%	866.12 mV	99.0%	1829	0.01%	36.24 ± 0.3%	311.0 ± 1.0
10	800	14.8%	1052.45 mV	99.3%	1749	0.02%	35.68 ± 0.2%	306.5 ± 0.5
11	820	3.9%	268.13 mV	96.8%	1065	0.01%	34.82 ± 0.4%	299.7 ± 1.0
12	850	10.2%	672.39 mV	98.6%	634	0.03%	32.96 ± 0.1%	284.8 ± 0.4
13	900	16.5%	1146.58 mV	98.8%	420	0.06%	34.74 ± 0.1%	299.1 ± 0.3
14	950	18.2%	1319.29 mV	99.2%	660	0.05%	36.34 ± 0.2%	311.8 ± 0.5
15	1000	4.0%	293.17 mV	97.4%	135	0.07%	36.37 ± 0.3%	312.0 ± 0.7
16	1020	0.8%	58.60 mV	71.2%	50	0.01%	34.68 ± 3.0%	298.5 ± 8.3
							total gas age:	301.2 ± 2.2

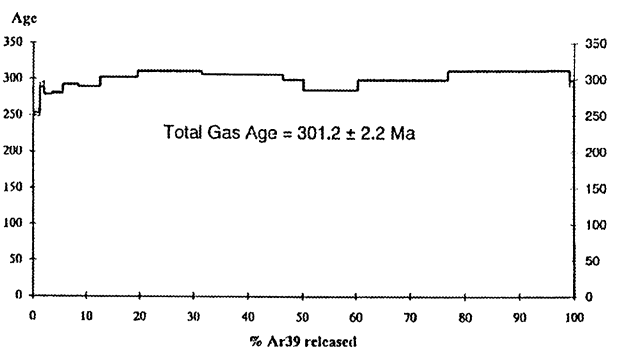

Fig. 6 (J, K, L) Ar/Ar plots

M) FR 745 m; MUSCOVITE, plagioclase gneiss (J = 0.004949 ± 0.4%)

Step	T[°C]	%39	40*	%rad	39/37	%36Ca	40*/39	age
1	650	0.5%	66.04 mV	85.9%	164	0.01%	30.72 ± 1.7%	266.8 ± 4.1
2	660	0.9%	119.74 mV	91.4%	319	0.01%	32.10 ± 1.4%	277.9 ± 3.7
3	670	1.0%	132.82 mV	93.5%	495	0.01%	32.96 ± 0.9%	284.8 ± 2.4
4	680	0.8%	109.57 mV	92.1%	485	0.01%	32.04 ± 1.2%	277.4 ± 3.0
5	700	1.3%	175.78 mV	95.0%	201	0.03%	31.50 ± 0.9%	273.1 ± 2.3
6	750	1.9%	266.89 mV	96.4%	601	0.01%	33.20 ± 0.7%	286.7 ± 1.8
7	780	3.5%	492.59 mV	97.3%	718	0.01%	33.74 ± 0.2%	291.1 ± 0.6
8	800	2.8%	402.99 mV	98.1%	789	0.02%	34.15 ± 0.3%	294.4 ± 0.7
9	820	3.2%	479.51 mV	98.1%	1233	0.01%	35.52 ± 0.1%	305.2 ± 0.3
10	850	11.5%	1769.09 mV	98.8%	2050	0.01%	36.70 ± 0.1%	314.6 ± 0.4
11	900	26.7%	4052.72 mV	99.3%	2591	0.02%	36.19 ± 0.2%	310.5 ± 0.5
12	920	9.3%	1325.46 mV	98.9%	1215	0.02%	33.81 ± 0.1%	291.7 ± 0.4
13	950	13.1%	1919.47 mV	98.9%	376	0.07%	34.90 ± 0.1%	300.3 ± 0.3
14	980	14.7%	2234.35 mV	99.3%	769	0.05%	36.33 ± 0.3%	311.7 ± 0.7
15	1000	7.0%	1078.78 mV	99.0%	681	0.04%	36.82 ± 0.2%	315.5 ± 0.6
16	1020	1.8%	289.15 mV	97.4%	1301	0.01%	37.95 ± 0.5%	324.4 ± 1.4
							total gas age:	305.4 ± 2.0

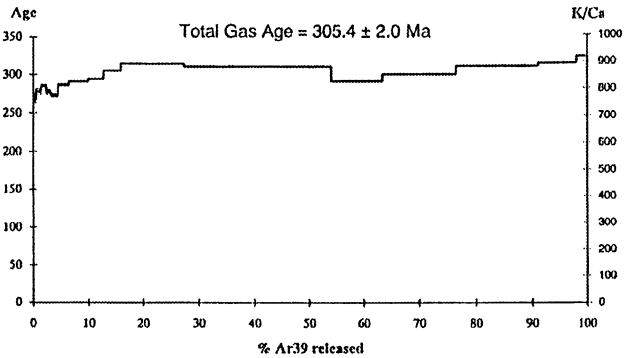

N) FR 745 m; BIOTITE, plagioclase gneiss (J = 0.004945 ± 0.4%

Step	T[°C]	%39	40*	%rad	39/37	%36Ca	40*/39	age
1	650	4.5%	783.81 mV	87.5%	113	0.02%	23.75 ± 1.4%	209.3 ± 2.8
2[1]	660	6.4%	1157.30 mV	94.9%	515	0.01%	24.62 ± 0.1%	216.6 ± 0.3
3[1]	670	4.6%	830.27 mV	96.7%	627	0.02%	24.56 ± 0.1%	216.1 ± 0.3
4[1]	680	4.7%	841.60 mV	97.3%	697	0.02%	24.39 ± 0.2%	214.7 ± 0.4
5[1]	710	4.5%	810.42 mV	97.5%	754	0.02%	24.41 ± 0.1%	214.8 ± 0.3
6[1]	730	7.1%	1283.41 mV	98.0%	808	0.02%	24.59 ± 0.3%	216.3 ± 0.6
7[1]	750	6.3%	1126.79 mV	98.0%	844	0.02%	24.34 ± 0.1%	214.2 ± 0.2
8[1]	780	7.1%	1275.52 mV	89.8%	735	0.00%	24.48 ± 0.2%	215.4 ± 0.4
9[1]	800	3.3%	619.89 mV	72.0%	508	0.00%	25.83 ± 0.5%	226.6 ± 1.0
10[1]	820	4.4%	844.15 mV	71.5%	361	0.00%	25.89 ± 0.6%	227.1 ± 1.3
11[1]	850	5.5%	970.68 mV	97.9%	263	0.07%	24.03 ± 0.2%	211.6 ± 0.4
12[1]	900	32.8%	5785.78 mV	98.1%	410	0.05%	24.01 ± 0.1%	211.5 ± 0.1
13	950	8.1%	1481.75 mV	90.4%	26	0.13%	24.90 ± 0.1%	218.9 ± 0.3
14	1000	0.6%	106.94 mV	72.3%	17	0.05%	26.02 ± 0.5%	228.2 ± 1.0
							total gas age:	214.9 ± 2.0
				87%			[1]plateau age:	213.5 ± 1.8

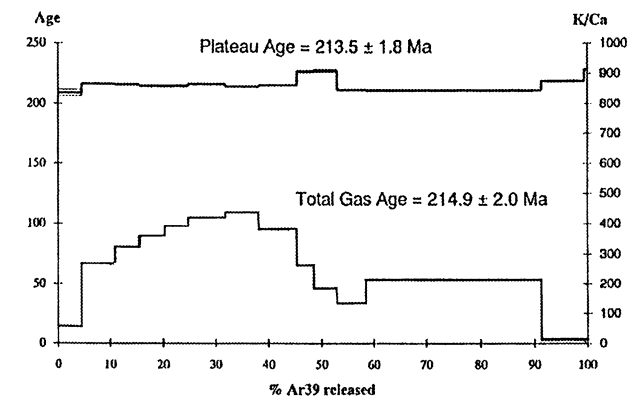

O) FR 747 m; MUSCOVITE, plagioclase gneiss (J = 0.004705 ± 0.4%)

Step	T[°C]	%39	40*	%rad	39/37	%36Ca	40*/39	age
1		3.9%	389.20 mV	93.0%	287	0.01%	31.16 ± 0.2%	257.8 ± 0.5
2		2.1%	230.74 mV	95.4%	425	0.01%	34.38 ± 0.6%	282.6 ± 1.7
3		1.8%	200.64 mV	96.0%	946	0.01%	35.04 ± 0.5%	287.6 ± 1.4
4		13.3%	1575.42 mV	97.0%	799	0.01%	36.73 ± 0.2%	300.5 ± 0.5
5		26.4%	3306.32 mV	98.8%	1316	0.02%	38.79 ± 0.1%	316.0 ± 0.2
6		12.8%	1505.78 mV	98.4%	1162	0.01%	36.42 ± 0.2%	298.1 ± 0.4
7		4.0%	464.91 mV	98.1%	713	0.02%	36.40 ± 0.1%	298.0 ± 0.1
8		7.9%	952.54 mV	98.2%	402	0.04%	37.17 ± 0.2%	303.8 ± 0.5
9		10.1%	1235.22 mV	98.9%	871	0.03%	38.04 ± 0.1%	310.3 ± 0.3
10		12.8%	1576.77 mV	99.2%	818	0.04%	38.18 ± 0.1%	311.4 ± 0.2
11		5.0%	638.54 mV	98.2%	407	0.03%	39.47 ± 0.1%	321.1 ± 0.4
							total gas age:	305.6 ± 1.8

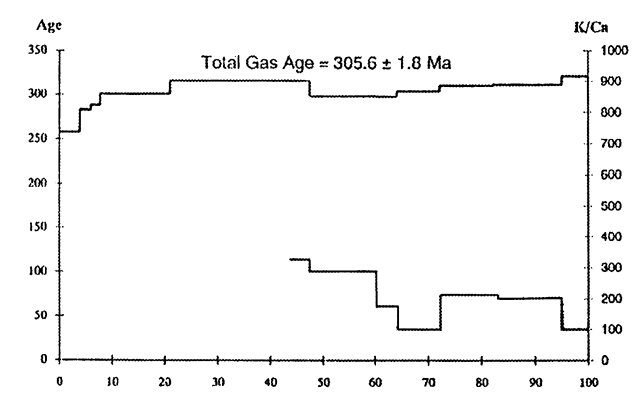

Fig. 6 (M, N, O) Ar/Ar plots

P) FR 1072 m; AMPHIBOLE, amphibolite (J = 0.004750 ± 0.4%)

Step	T[°C]	%39	40*	%rad	39/37	%36Ca	40*/39	age
1	720	7.0%	84.24 mV	41.3%	0.07	2.67%	32.41 ± 3.0%	269.9 ± 7.5
2	730	3.9%	47.86 mV	35.5%	0.06	2.38%	32.79 ± 3.6%	272.9 ± 9.1
3	740	3.9%	51.38 mV	79.0%	0.06	14.26%	35.84 ± 15.2%	296.3 ± 41.8
4	800	29.9%	433.10 mV	90.0%	0.05	28.43%	39.29 ± 1.3%	322.6 ± 3.8
5	840	12.4%	177.71 mV	89.0%	0.06	24.87%	38.91 ± 0.4%	319.7 ± 1.3
6	860	8.8%	135.26 mV	89.4%	0.04	32.13%	41.67 ± 1.1%	340.4 ± 3.6
7	910	23.1%	392.42 mV	89.6%	0.04	31.30%	46.36 ± 0.3%	375.2 ± 0.9
8	950	9.6%	201.11 mV	78.2%	0.03	14.75%	56.93 ± 0.7%	451.2 ± 2.6
9	1000	1.4%	31.13 mV	67.3%	0.03	10.18%	61.91 ± 8.7%	485.9 ± 37.1
								343.9 ± 12.2

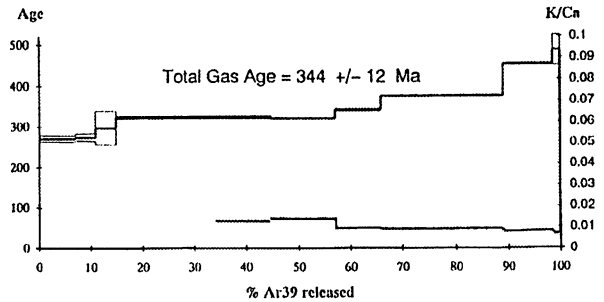

Fig. 6 (P) Ar/Ar plots

Ar/Ar: slightly disturbed plateau pattern (former age >325 Ma) with a saddle and low-temperature Ar loss (Permian?)

745 m. Muscovite–plagioclase gneiss, preserved pre-Alpine structure.

Muscovite: coarse flakes.

Rb/Sr: 286,8±3, spread only 7.4.

Ar/Ar: disturbed (saddle) plateau pattern, former age >315 Ma with Permian? low-temperature Ar loss.

Biotite: coarse pre-Alpine flakes with Ti and sphene unmixing.

Rb/Sr: 108±3 Ma, spread 286.

Ar/Ar: well developed plateau pattern, 213 Ma with a small horst at intermediate temperatures (uniform excess Ar).

742 m. Same lithology as 745 and 747 m.

Muscovite: Ar/Ar rejuvenated plateau type (>300 Ma.)

720 m. Muscovite–biotite plagioclase gneiss, well preserved pre-Alpine structure, strong fluid-driven alteration of plagioclase, sphene unmixing in biotite, new formation of a few chlorite flakes.

Muscovite: Ar/Ar: 240±3.7 Ma with a saddle shaped pattern.

Biotite: Ar/Ar: 171.3 Ma±2.1 Ma plateau type, partially reset?

609 m. Small wedge of tectonically intercalated fine-grained biotite gneiss with preserved sedimentary layering. Form relics of pre-Alpine biotite porphyroblasts with sphene unmixing.

Biotite: Ar/Ar: plateau type 178 Ma.

327 m. Microcline augengneiss.

Muscovite: coarse-grained relics.

Rb/Sr: 294±3 Ma. (extreme spread 1110).

Ar/Ar: well preserved plateau type, 184 Ma with minor low temperature argon loss.

325 m. Microcline augengneiss as described under 327 m.

Muscovite: Ar/Ar: 98±1 Ma, slightly disturbed plateau type.

Biotite: 93±1 Ma, well preserved plateau type.

276 m. Phyllitic micaschist (biotite-muscovite)

Muscovite: relic flakes were separated.

Ar/Ar: slightly discordant saddle shaped age pattern (total gas 225 Ma), lowest age step at 170 Ma.

Biotite: no relics, newly formed grains, coarse fraction.

Ar/Ar: plateau type, erratic at high temperature steps, 256 Ma.

210 m. Muscovite phyllite with distinct structural reworking.

Muscovite: Ar/Ar 142±1.4 Ma, disturbed saddle

Table 3

Apatite and zircon fission-track analytical results

	Depth	Cryst.	Ps	(Ns)	Pi	(Ni)	P(χ^2) [%]	FT age [Ma±2s]	Track length (n) [µm]
Apatite ages									
	184 m	33	5.83	(872)	12.2	(2074)	<1	46.2±4.8	14.0±0.8 (8)
	276 m	25	3.39	(729)	7.92	(1752)	30	42.4±4.6	13.9±0.9 (23)
	327 m	35	1.61	(362)	3.94	(894)	5	41.4±5.8	
	609 m	15	3.29	(360)	4.17	(495)	11	42.1±6.6	
	720 m	20	5.46	(910)	13.4	(2221)	18	40.5±4.1	13.8±1.0 (100)
	1047 m	14	0.08	(16)	0.30	(63)	–	25.4±14.3	
	1087 m	20	5.57	(1117)	12.1	(2440)	12	45.3±4.4	13.4±1.1 (50)
Zircon ages									
	327 m	16	100.0	(1429)	52.4	(759)	<1	54.2±6.5	
	1047 m	15	59.0	(1639)	28.7	(806)	11	57.8±6.8	
	1087 m	16	70.2	(1355)	33.9	(614)	3	61.8±7.7	

Cryst: number of dated crystals
Ps, Pi: spontaneous and induced track density [x10^5 tr./cm^2]
Ns, Ni: number of spontaneous and induced tracks counted
P(χ^2) probability obtaining Chi-square value for n degree of freedom (where n=No of crystals-1)

shaped pattern with possible excess Ar in low temperature steps. Due to the missing spread in the Rb/Sr system no meaningful age calculation for the white micas was possible.

185 m. Biotite-muscovite phyllite.

Muscovite: coarse flakes.

Ar/Ar: saddle shaped pattern, highest ages 215 Ma, no single step below 178 Ma.

Biotite: coarse flakes, intergrown with muscovite, sphene unmixing, perfectly annealed.

Rb/Sr: 72±4 Ma., spread WR/B=119.

Discussion of age results

The polymetamorphic history clearly visible meso- and microscopically is reflected also in the geochronological data. The lower unit yielded ± well preserved Variscan Rb/Sr ages of muscovites (338, 286±3 Ma) from the plagioclase gneisses. 294±3 Ma was obtained on a highly radiogenic muscovite from a microcline augengneiss from the upper unit.

We assume that 338±4 is still close to the former Variscan cooling age. The analytically distinctly younger ages up to 286 Ma most probably can be attributed to the limited spread and especially in the case of 327 m due to partial opening in the consequence of deformation induced annealing and recrystallization. KOVÁCH & SVINGOR (1981) reported well defined ages of pegmatitic muscovites of 351±9 Ma, and three more muscovites with a spread <10 also fit to the same reference line. We have no information if these samples belong to the lower unit rather than to the upper one. However the reason for these older ages preferentially may be their bigger primary grainsize. It is well known that even low grade amphibolite facies temperatures may not be sufficient to reset a cm-size white mica completely.

The microcline augengneiss at 327 m is highly radiogenic (Rb^{87}/Sr^{85} 51.6), so a whole rock age of 438 Ma can be calculated. This "single sample" Rb/Sr age may be considered with caution but it indicates that Early Palaeozoic acid magmatic rocks are associated in this crystalline unit. Dr. KOVÁCH kindly provided us with an unpublished report on the granite gneisses of the Sopron area, where he found arguments for an Early Palaeozoic protolith age.

Only one amphibole (1072 m) from the lower unit was investigated. Ages of 323–375 Ma for the 820–950 °C steps agree roughly with the Rb/Sr white mica ages. We cannot be sure, if the low-teperature ages of 270 Ma are only due to thermal resetting of the amphibole. The high K/Ca ratio of these steps make it possible that some tiny biotite inclusions could be responsible. The K/Ca ratio also indicates a chemical zonation of the amphibole. Ages of >450 Ma from the highest temperature steps were obtained. These high ages of core domains give a weak argument for a pre-Variscan age of this fine-grained gabbroic rock.

Fission track measurements (results and interpretation)

Fission track measurements were performed on apatites coming from seven samples and on zircons from three samples; analytical results are shown in Table 3. The ages are distributed in a narrow range (43.0±2.3 Ma). As there is no relationship between the depth of the samples and the obtained ages, the formation of ages was rather a rapid than a slow process, as the track length result support it. Each sample shows a significant, but not too great track shortening. The track populations do not contain strongly shortened tracks, thus the apparent apatite ages express the termination of the cooling process, which was started by the Late Cretaceous thrusting.

The thermal history was modelled by the programs of WILLETT (1992) and GALLAGHER (1993). The results of the modelling is shown in fig. 7. Only one geological control exists on the uplift-burial history of the Fertőrákos area: the beginning of the post-metamorphic sedimentation in Early/Middle Miocene during Karpatian (-17 Ma). Thus for the 17–15 Ma period we have assumed surface temperatures. The envelope of the acceptable thermal path consists of three parts:

I. The cooling during Paleocene–Early Eocene was probably monotonous until the temperature around 50 °C in Middle Eocene. This period can be characterized by a narrow t/T field.

2. The Eocene–Miocene thermal history of the studied rocks is questionable, but the temperature was less, than 55 °C. A young thermal overprint hides the details of the thermal path before the Miocene.

3. The generally mild shortening of the tracks is the consequence of a post-Karpatian burial. The final warming and rapid cooling took place during the last 14–8 Ma. Maximum temperatures were in the range of 45–65 °C between Badenian and Quaternary.

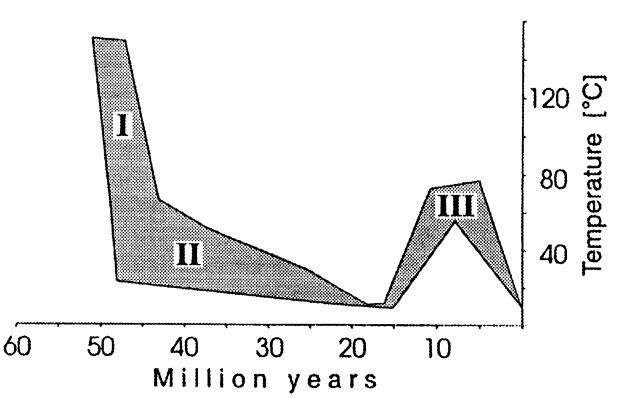

Fig. 7. Post-Cretaceous thermal history of the Fertőrákos block based on the modelling of the fission track data

I. Rapid cooling in Early–Middle Eocene, II. "Stagnation period" during Late Paleogene-Early Miocene, III. Sediment burial and erosion during Late Neogene

The Lower-Austroalpine crystalline nappes are covered by syn- and post-extensional sedimentary sequences in the nearby Rába basin. In some sub-basins Miocene sediment thickness exceeds 2000 m (FÜLÖP 1990). The subsidence of these zones could have been similar to the subsidence of the Fertőrákos block, but it was followed there by a very young uplift and erosion at the zone of Alpine foothills. This exhumation at the western margin of the Pannonian basin system is related to the Pliocene- to recent change of the stress-field of the entire regime (HORVÁTH & CLOETHING 1994). Young uplift of similar size and age was also reported from the northern margin of the Pannonian basin by DUNKL et al. (1994).

Geological significance of the thermal history in the regional framework

An important result of our investigation of this borehole was the finding that the lower portion, lithologically comparable to the Wechsel plagioclase gneisses yielded more or less preserved Variscan white mica cooling ages. This result is in good agreement with MÜLLER (1994) who was able to demonstrate an Early Variscan high pressure event in the Wechsel gneisses and a Late Variscan, Permian overprint.

Our $^{39}A/^{40}Ar$ results from the coarse-grained white micas from the Wechsel gneisses yielded usual Late Variscan cooling ages around 300–305 Ma, which are slightly affected by a later thermal overprint visible in the saddle shaped age pattern. The lower temperature steps are distinctly younger, but there was not a single step recognized below 250 Ma (samples 742, 745, 747, 1072) except the sample 720, which suffered a stronger rejuvenation. In comparison with the results of MÜLLER we interpret this as an argument for a Permian overprint of this unit. We found one biotite from sample 745, of which Rb/Sr system has been rejuvenated broadly to Cretaceous values (108±1 Ma).

MÜLLER demonstrated that the Alpine deformation in the Wechsel unit is concentrated in rather thin shear zones and dated them 86±12 Ma. Our observation of several thin sections from this lower unit corroborate this picture.

The upper unit, lithologically and structurally comparable to the Semmering unit, is characterized by a strong structural reworking within low to medium greenschist facies. The tectonic contact to the lower unit is complicated and contains several variegated intercalations.

Based on our studies of thin sections we assume that large rock volumes were recrystallized in Early Alpine times. Contrary to this straightforward interpretation of the thin sections, the $^{39}Ar/^{40}Ar$ results of the white micas of this unit are not easy to interpret. Most of the samples yielded "mixed" ages in the range 142–225 Ma. Excess argon obviously plays a major role in this whole unit. This is indicated by the sample 276 m (a well recrystallized phyllitic micaschist), from which the biotite yielded a plateau-type age pattern of 256±1.6 Ma, which is distinctly higher than the $^{39}Ar/^{40}Ar$ age of the coexisting white mica of about 225 Ma. The excess Ar of this biotite shows a uniform distribution.

Only in one sample out of six we found Cretaceous ages on both micas. Whether these ages (muscovite 98 Ma, biotite 93 Ma) represent true cooling ages or may also be affected by a small amount of excess Ar, is difficult to assess. In the light of the available regional geochronological information the latter case is more probable.

The complicated saddle-shaped age pattern of white micas of the samples 184, 210 and 276 m are difficult to interpret, but we assume a complex history. The high temperature steps may indicate domains which have not been fully reset and the low temperature portion on the age diagram is probably a combination of excess Ar and later diffusional loss. It should be mentioned that even the lowest temperature steps do not show usual Cretaceous values.

Unfortunately the Rb/Sr information is limited. One biotite from 184 m gave a late Cretaceous cooling age of 72 Ma. Due to the lacking spread it was not possible to calculate a reliable age of the white mica fraction of the sample 210 m.

The 294±3 Ma age data of the white mica from a microcline augengneiss (327 m) bears a problem in respect to our interpretation, that the fabric of this rock is dominated by Alpine recrystallization. The reason for this is that coarse-grained relictic micas were enriched during separation.

Although we were not able to get a precise geochronological information about the time of the Early Alpine overprint, the presence of excess argon in large rock volumes in the rocks of the lowermost Lower Austroalpine Units (LAA) is a useful information. It means, that during thrusting of the LAA nappes over the Wechsel unit large amounts of radiogenic argon migrated together with the released fluids from below along the tectonically active deformational zones and were incorporated in the contemporaneously cooling minerals. It is a characteristic feature that this excess argon is usually found close to the thrust plane and is not recognized in higher levels. From the LAA realm in Sopron, which represents a tectonically higher position compared to the rock unit in the investigated borehole, BALOGH & DUNKL (1994) reported a series of K/Ar data which do not indicate the incorporation of major amounts of excess argon.

HUBER (1994) dated leukophyllites from several occurrences within the LAA crystalline, including Rabenwald, and many other localities, and he found $^{39}Ar/^{40}Ar$ cooling ages of white micas in the range 72–96 Ma with a distinct clustering of data around 87 Ma.

From this geochronological information it seems reasonable that the whole LAA crystalline in the Semmering system has seen an intense Early Alpine tectonism and metamorphism. Most probably the same event has affected the Permo–Mesozoic intercalations in this area, which is checked at the moment in detail in several localities. It means that in the Semmering System the Early Alpine continental margin was overridden by the main mass of Austroalpine crystalline of Kor- and Saualm and comparable units. It should be mentioned that the metamorphic overprint of the LAA Mesozoic in the Radstädter Tauern was an Early- to Late Tertiary process (SLAPANSKY & FRANK 1987). It means that further to the west the LAA units have seen later tectonism and metamorphism than in the Semmering area.

The more or less preserved Variscan structures and ages from the Wechsel unit indicate that this unit has seen distinctly lower temperatures as the overriding LAA units. They represent therefore the frontal parts of the Austroalpine crystalline wedge, which always had a high structural position.

It may be mentioned that a similar history can be deduced for the occurrences of metamorphic rocks of the Subtatricum unit from Wolfsthal belonging to the Little Carpathians south of the Danube, where mineralogically perfectly preserved Variscan assemblages and biotite $^{39}Ar/^{40}Ar$ cooling ages up to 317 Ma are known (pers. comm. A. HAMID).

Acknowledgements

GYÖNGYI LELKES-FELVÁRI acknowledges financial support from Büro für Austauschprogramme mit Mittel und Osteuropa, Wien, Aktion Österreich–Ungarn, Wissenschafts- und Erziehungskooperation, Projekt 10ö1, 12ö15 and from Hungarian Scientific Research Fund (OTKA) No 3002 and No 7211. Fission track measurements were performed in the framework of Hungarian Scientific Research Fund (OTKA) 232/91. We are grateful to the former Mecsek Ore Mining Company, Pécs for providing samples and thin sections.

REFERENCES

BALOGH KAD. & DUNKL I. 1994: K/Ar and fission track dating of metamorphic rocks from the Sopron Mts., Lower Ausroalpine unit, Hungary. — Mitt. Öst. Min. Ges. 139, 26–27. Conference Preprint. Pre-Alpine crust in Austria.

DUNKL I., ÁRKAI P., BALOGH K., CSONTOS L. & NAGY G. 1994: A hőtörténet mod llezése fission track adatok e felhasználásával — a Bükk-hegység kiemelkedéstörténete. (Thermal modelling based on apatite fission track dating: the uplift history of the Bükk Mts., Inner Western Carpathians, Hungary).-Földt. Közl. in press

FAUPL P. 1972: Zur Geologie und Petrographie des südlichen Wechselgebietes. — Mitt. Geol. Ges. 63, 22–51.

FRANK W. et al. in prep.

FUCHS W. 1965: Geologie des Ruster Berglandes (Burgenland). — Jb. Geol. B. A. 108, 155–194.

FÜLÖP J. 1990: Magyarország geológiája (Geology of Hungary) Paleozoikum I. — Budapest. 325 p.

GALLAGHER K. 1993: Monte Trax, a fission track thermal history modelling program for Macintosh. Manuscript Software Manual, 30 p.

HORVÁTH F. & CLOETHING S. 1994: Tectonic reactivation of the Pannonian basin during the Quaternary — in press.

HUBER M. 1994: Untersuchungen an Leukophyllit-Vorkommen im Unterostalpin. Diss. Montanuniversitat Leoben.

KÓSA L. & FAZEKAS V. 1981: Geologisch-petrographischer Aufbau des kristallinen Schieferkomplexes von Fertőrákos (Sopron Gebirge, Westungarn). — Földt. Közl. 111, 424–452.

KOVÁCH Á. & SVINGOR É. 1981: On the age of metamorphism in the Fertőrákos metamorphic complex, NW. Hungary. — Verh. Geol. B. A., 73–81.

KOVÁCH Á. & SVINGOR É. 1988: A Rb/Sr age study of crystalline rocks in the Sopron Mts., Western Hungary. — Proceeding reports of the XIII-th Congress of KBGA. Cracow, 483–484.

LELKES-FELVÁRI GY., SASSI F. P. & VISONÁ D. 1984: Pre-Alpine and Alpine developments of the Austridic basement in the Sopron area (Eastern Alps, Hungary). — Rendiconti Soc. Ital. Min. Petr. 39, 593–612.

MÜLLER W. 1994: Neue geochronologische und strukturgeologische Daten zur geodynamischen Entwicklung des nördlichen Semmering- und Wechselgebietes (Niederösterreich). — Dissertation Univ. Wien

SAMSON S. D. & ALEXANDER E. C. 1987: Calibration of the interlaboratory 40 Ar/39 Ar dating standard, MM hb-1. — Chemical Geology 66, pp. 27–34.

SLAPANSKY P. & FRANK W. 1987: Structural evolution and geochronology of the northern margin of the Austroalpine in the northwestern Schladming crystalline (NE Radstadter Tauern) — in: FLÜGEL H. W. & FAUPL P. (eds): Geodynamics of the Eastern Alps, Vienna (Deuticke), 244–262.

WILLET S. D. 1992: Modelling thermal annealing of fission tracks in apatite. — In: ZENTILLI M. & REYNOLDS P. H. (eds.): Short course handbook on low temperature thermochronology (Min. Assoc. Canada), 43–72.